Chapter 3.

SPACE-VECTOR PWM

3.1. Space-Vector Modulation

3.1.1. Three-Dimensional Vector Representation

A multilevel converter can synthesize output voltages from many discrete voltage levels. Therefore, the functional diagram of an n-level diode-clamped converter can be represented as shown in Fig. 3.1.
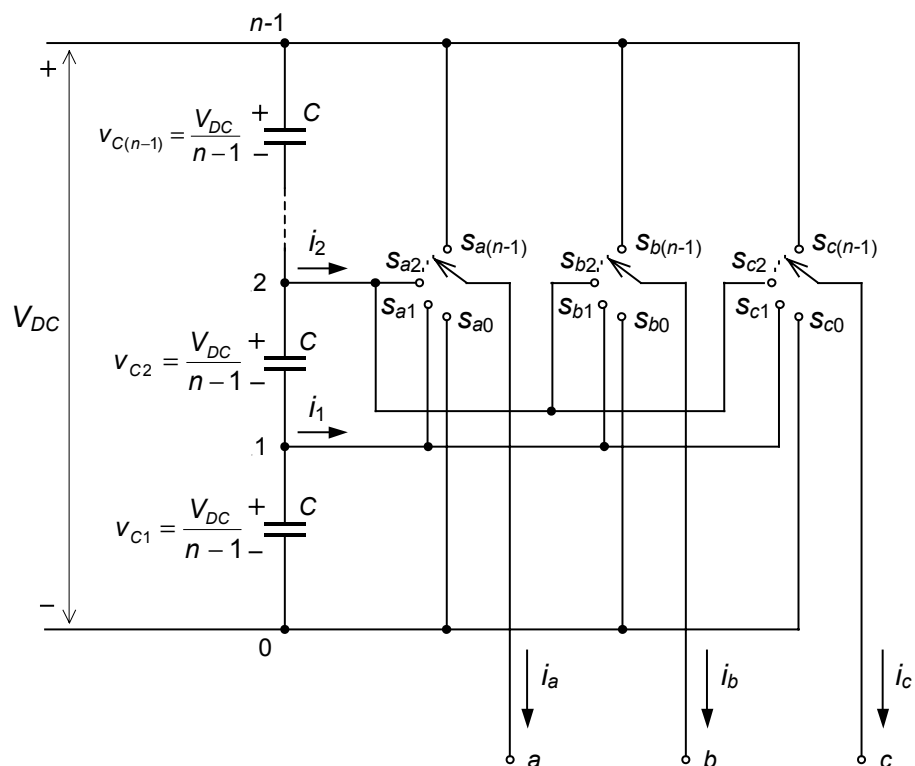

Fig. 3.1. *Functional diagram of an n-level diode-clamped converter.*

Each switching state, or combination of phase-leg switches, produces a defined set of three-phase voltages, which can be represented as vectors in the three-dimensional Euclidean diagram (Fig. 3.2) [A26].
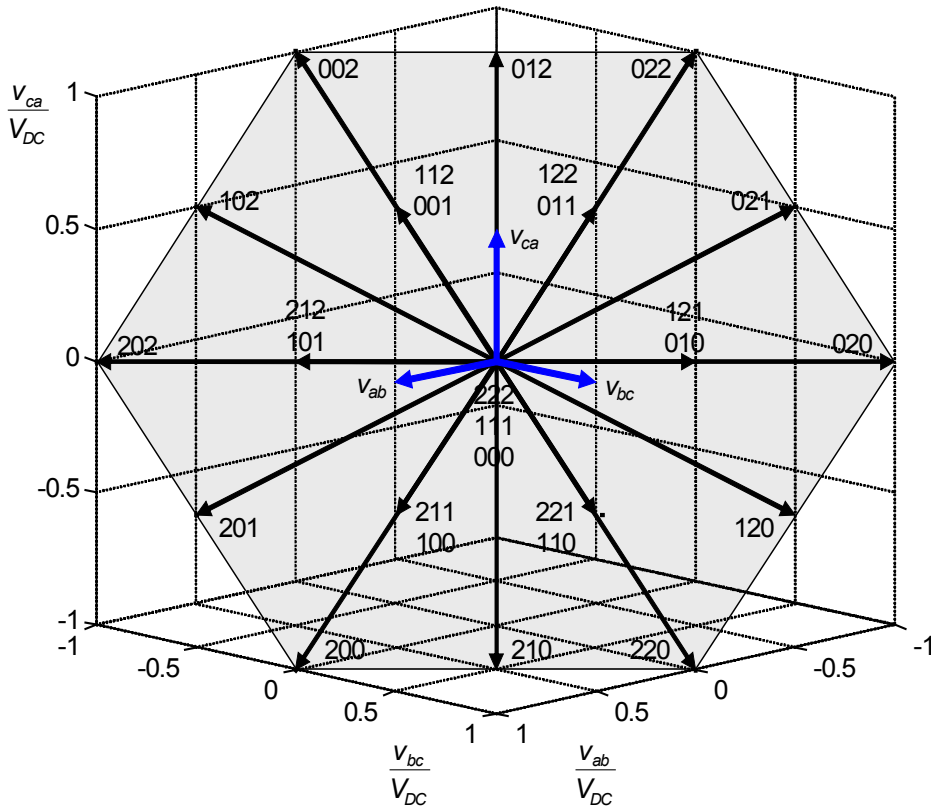

Fig. 3.2. *Three-dimensional SV diagram.*

The variables represented in Fig. 3.2 are the line-to-line voltages from a three-level converter, as follows:

$$\vec{\mathbf{V}} = [v_{ab} \quad v_{bc} \quad v_{ca}]^{\top}, \quad \text{or} \quad \vec{\mathbf{V}} = \frac{V_{DC}}{n-1}[i-j \quad j-k \quad k-i]^{\top}, \tag{3.1}$$

where i, j, $k \in [0, \ldots , n\text{-}1]$, which define the position of the single-pole n-throw switches of phases a, b and c, respectively. The vectors are labeled as (i, j, k) in order to simplify their notation.

Because of Kirchof's Law, the sum of the line-to-line voltages is always zero; this is really an equation of the plane in the line-to-line coordinate system. This means that all of the vectors of a multilevel converter lie in a plane, and that is how they are usually represented.

When the phase voltages are represented in the three-dimensional diagram, they do not lie in a plane. However, they can be projected into a plane, thereby representing an equivalent two-dimensional diagram.

Coming back to the three-dimensional representation, a voltage reference vector ($\vec{m}$) that must be synthesized by PWM-averaged approximation can also be represented in vector form, as follows:

$$\vec{m} = \hat{V}_{LL} \begin{bmatrix} \cos(\omega t + \theta_o) \\ \cos(\omega t - \frac{2\pi}{3} + \theta_o) \\ \cos(\omega t + \frac{2\pi}{3} + \theta_o) \end{bmatrix}, \tag{3.2}$$

where $\hat{V}_{LL}$ is the amplitude of the line-to-line voltages. Since this vector has only two degrees of freedom, it also lies on the same plane as the switching vectors. Using the definition of vector norm, the length of the reference vector is

$$\left| \vec{m} \right| = \sqrt{\left| \vec{m} \right|^2 + \left| \vec{m} \right|^2} = \sqrt{\frac{3}{2}} \hat{V}_{LL}, \tag{3.3}$$

while by the same definition, the length of the longest switching vector is

$$\left| \vec{V}_{max} \right| = \sqrt{2}\, V_{DC}. \tag{3.4}$$

The maximum length of the reference vector (3.3) that can be synthesized in steady-state conditions equals the radius of the largest circle that can be inscribed in the outer hexagon. Therefore, the maximum length of the reference vector is

$$\left| \vec{m}_{max} \right| = \frac{\sqrt{3}}{2} \left| \vec{V}_{max} \right|. \tag{3.5}$$

By substituting (3.4) into (3.5) and comparing the resulting equation with (3.3), the maximum amplitude of the undistorted line-to-line voltage that can be synthesized is

$$\hat{V}_{LL\,max} = V_{DC}. \tag{3.6}$$

3.1.2. Two-Dimensional Vector Representation

The Clarke's Transformation [B12, B13] allows the three-dimensional vector representation to be displayed in a two-dimensional diagram. Given three output voltages of the converter (v_{a0}, v_{b0} and v_{c0}), the projection in a plane $\alpha\beta$ (v_α, v_β) of a three-dimensional vector is

$$\vec{V} = v_\alpha + j\,v_\beta = v_{a0}\,\vec{a}^0 + v_{b0}\,\vec{a}^1 + v_{c0}\,\vec{a}^2 \,, \tag{3.7}$$

where $\vec{a} = e^{j\frac{2\pi}{3}}$.

Fig. 3.3(a) shows the three unitary director vectors of this transformation, while Fig. 3.3(b) shows an example for the case in which v_{a0}=200 V, v_{b0}=300 V, and v_{c0}= -100 V.
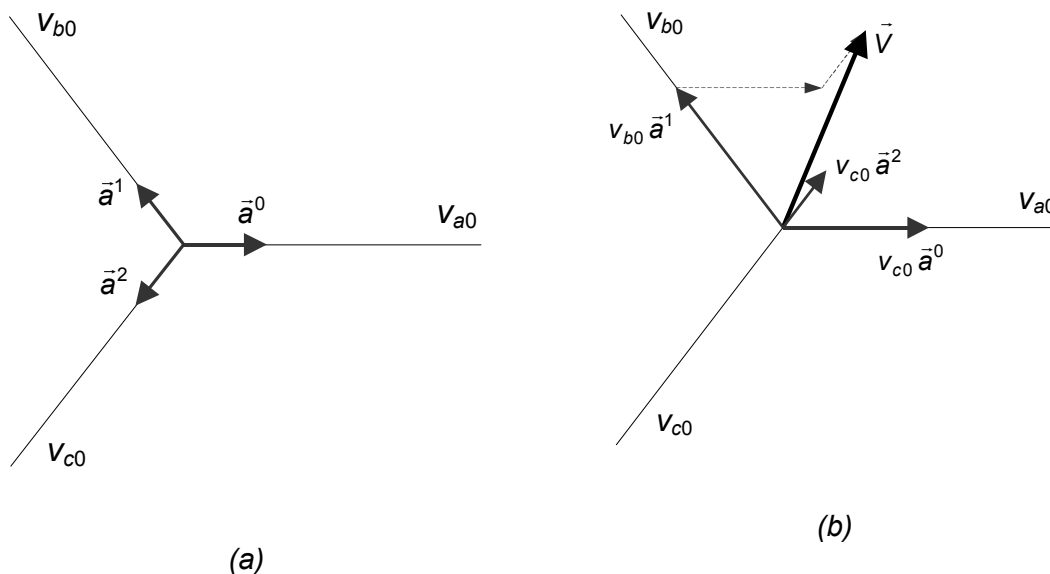

(a)

(b)

Fig. 3.3. *Clark's Transformation: (a) director vectors, and (b) example of spatial vector for v_{a0}=200 V, v_{b0}=300 V, and v_{c0}=-100 V.*

The aim of the SVM is to generate a reference vector ($\vec{m}$) in the same plane for each modulation cycle. As the reference vector may not be the same as any vector produced by the converter, its average value can be generated using more than one vector per modulation cycle by PWM-averaged approximation. Selecting proper vectors and applying them in a suitable order helps the devices achieve low switching frequencies.

In steady-state conditions, the reference vector rotates at a constant angular speed (ω), which defines the frequency of the output voltages. The amplitude of the fundamentals of those voltages is proportional to the length of the reference vector.

There are eight possible states for the two-level converter ($n^3 = 2^3 = 8$), which produce the voltage vectors shown in Fig. 3.4. Six of these vectors have equal lengths and are located every sixty degrees (100, 110, 010, 011, 001, 101). The other two vectors are in the origin because of their null lengths (000, 111).
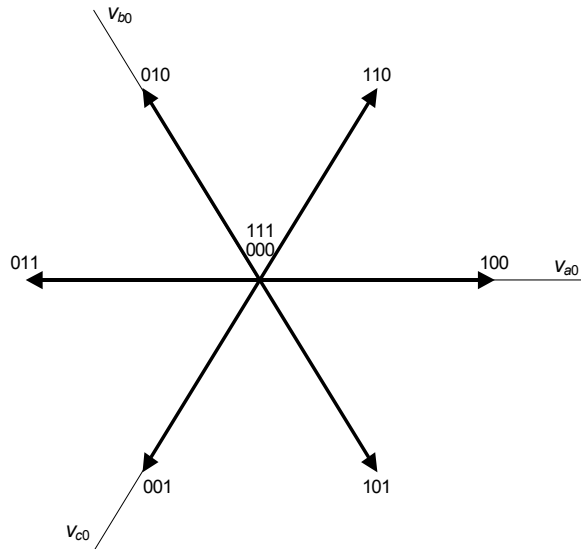

Fig.3.4. *SV diagram of the two-level converter.*

The SV diagrams of the three-level and four-level converters have twenty-seven and sixty-four vectors, respectively (Fig. 3.5).
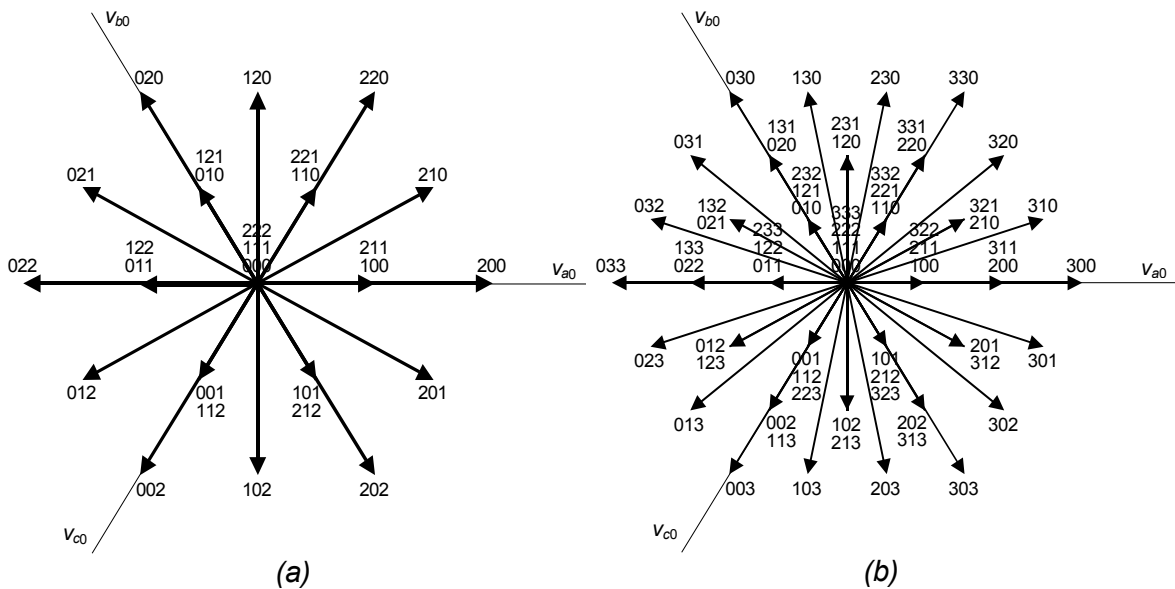

(a)   *(b)*

Fig.3.5. *SV diagrams of (a) the three-level converter, and (b) the four-level converter.*

The redundant vectors in the diagram produce the same line-to-line voltages. The three-level converter has six double vectors and one triple vector in the origin. The four-level converter has twelve double vectors, six triple vectors and one tetra

vector in the origin. Proper utilization of these vectors will help the voltages of the capacitors to achieve balance.

3.1.3. Limiting Area

Any set of three vectors $\vec{v}_1$, $\vec{v}_2$ and $\vec{v}_3$ in a plane ($\alpha\beta$ in Fig. 3.6) can generate any reference vector $\vec{m}$ in the same plane using PWM-averaged approximation, if the reference vector lies in the triangle connecting the tips of $\vec{v}_1$, $\vec{v}_2$ and $\vec{v}_3$.
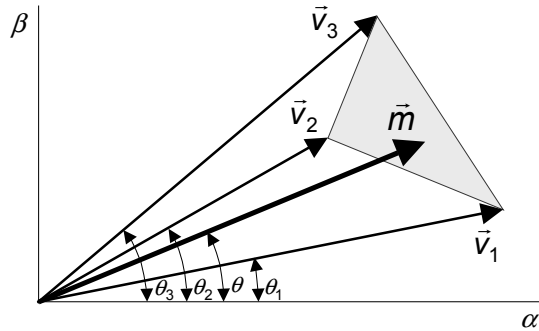

Fig. 3.6. *Limiting area to generate the reference vector ($\vec{m}$) by using three vectors.*

The average reference vector can be obtained by sequentially applying these vectors in a modulation period in accordance with

$$\frac{1}{T_m}\int_0^{T_m}\vec{m}\,dt = \frac{1}{T_m}\int_0^{T_1}\vec{v}_1\,dt + \frac{1}{T_m}\int_{T_1}^{T_1+T_2}\vec{v}_2\,dt + \frac{1}{T_m}\int_{T_1+T_2}^{T_m}\vec{v}_3\,dt\,, \qquad (3.8)$$

where T_m is the modulation period, and $T_1+T_2 \leq T_m$.

Assuming that $\vec{m}$ remains approximately constant during a modulation period, which is acceptable if T_m is much smaller than the line period (T), then (3.8) can be approximated as:

$$\vec{m} = d_1\vec{v}_1 + d_2\vec{v}_2 + d_3\vec{v}_3\,, \qquad (3.9)$$

in which d_1, d_2 and d_3 are the duty cycles of vectors $\vec{v}_1$, $\vec{v}_2$ and $\vec{v}_3$, respectively. They must satisfy the following condition:

$$d_1 + d_2 + d_3 = 1. \qquad (3.10)$$

The boundaries of the area that allows the reference vector to be generated can be determined assigning zero value to one of the duty cycles. For example, imposing d_3=0, and by means of (3.9) and (3.10), the vector $\vec{m}$ can be expressed as follows:

$$\vec{m} = \vec{v}_2 + d_1(\vec{v}_1 - \vec{v}_2) . \tag{3.11}$$

As all the duty cycles could potentially utilize values in the interval $[0, 1]$, the tip of the reference vector is on the line that joins the extremes of the vectors $\vec{v}_1$ and $\vec{v}_2$ (Fig. 3.7), which can be verified by simply making d_1 vary within that interval. Therefore, this segment is one boundary of the limiting area. The other two remaining segments of the triangular region in Fig. 3.6 can be determined by assigning zero to d_1 and d_2 separately.
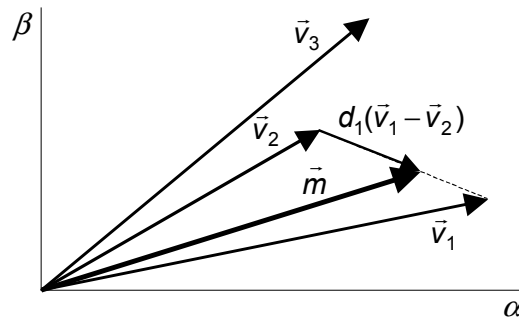

Fig. 3.7. *Boundary of the area, determined when d_3=0.*

Any reference vector outside of this area requires that one or more duty cycles be negative. This fact does not make physical sense; thus, it cannot be generated by this set of three vectors.

3.1.4. Calculation of Duty Cycles

Equation (3.9) can be expressed by the following exponential notation:

$$\vec{m} = me^{j\theta} = d_1 v_1 e^{j\theta_1} + d_2 v_2 e^{j\theta_2} + d_3 v_3 e^{j\theta_3} ; \tag{3.12}$$

therefore, the duty cycles of the vectors can be calculated according to either of the following equation systems:

$$\begin{bmatrix} d_1 \\ d_2 \\ d_3 \end{bmatrix} = \begin{bmatrix} v_1\cos\theta_1 & v_2\cos\theta_2 & v_3\cos\theta_3 \\ v_1\sin\theta_1 & v_2\sin\theta_2 & v_3\sin\theta_3 \\ 1 & 1 & 1 \end{bmatrix}^{-1} \begin{bmatrix} m\cos\theta \\ m\,sen\theta \\ 1 \end{bmatrix}, \tag{3.13}$$

or

$$\begin{bmatrix} d_1 \\ d_2 \\ d_3 \end{bmatrix} = \begin{bmatrix} \mathrm{Re}(\vec{v}_1) & \mathrm{Re}(\vec{v}_2) & \mathrm{Re}(\vec{v}_3) \\ \mathrm{Im}(\vec{v}_1) & \mathrm{Im}(\vec{v}_2) & \mathrm{Im}(\vec{v}_3) \\ 1 & 1 & 1 \end{bmatrix}^{-1} \begin{bmatrix} \mathrm{Re}(\vec{m}) \\ \mathrm{Im}(\vec{m}) \\ 1 \end{bmatrix}. \tag{3.14}$$

In general terms, given any bi-dimensional stationary base frame, orthogonal or not, the expression would be:

$$\begin{bmatrix} d_1 \\ d_2 \\ d_3 \end{bmatrix} = \begin{bmatrix} \left.\vec{v}_1\right|_x & \left.\vec{v}_2\right|_x & \left.\vec{v}_3\right|_x \\ \left.\vec{v}_1\right|_y & \left.\vec{v}_2\right|_y & \left.\vec{v}_3\right|_y \\ 1 & 1 & 1 \end{bmatrix}^{-1} \begin{bmatrix} \left.\vec{m}\right|_x \\ \left.\vec{m}\right|_y \\ 1 \end{bmatrix}. \tag{3.15}$$

The calculation process for any of these equation systems requires inverting a matrix, which complicates the application of this method to a real-time processor system. Additionally, the equation system may need to be solved more than once per modulation period (T_m), since the region where the reference vector lies is previously unknown. A simplified mathematical process should be found.

3.1.5. Calculation of Duty Cycles by Projections

A general method for calculating duty cycles of vectors is explained in this section. This method is based on determining some projections of the reference vector, and it will be applied in order to simplify the modulation process later.

The vectors $\vec{p}_1$ and $\vec{p}_2$ in Fig. 3.8 are the projections from the reference vector $\vec{m}$ onto the segments that join the extreme of $\vec{v}_3$ to $\vec{v}_1$ and to $\vec{v}_2$, respectively.
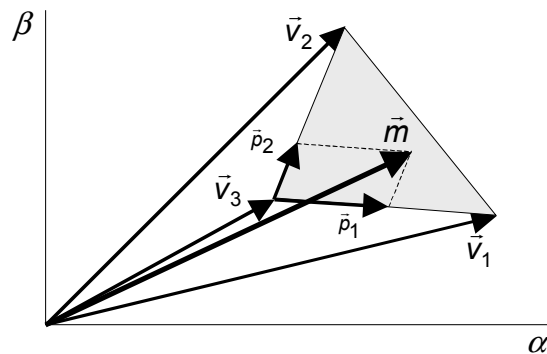

Fig. 3.8. Projections of the reference vector $\vec{m}$ ($\vec{p}_1$ and $\vec{p}_2$).

Therefore, the reference vector can be expressed as follows:

$$\vec{m} = \vec{p}_1 + \vec{p}_2 + \vec{v}_3 \tag{3.16}$$

or

$$\vec{m} = p_1 \frac{\vec{v}_1 - \vec{v}_3}{l_1} + p_2 \frac{\vec{v}_2 - \vec{v}_3}{l_2} + \vec{v}_3 , \tag{3.17}$$

where l_1 and l_2 are the lengths of the vectors $\vec{v}_1 - \vec{v}_3$ and $\vec{v}_2 - \vec{v}_3$, respectively. Finally, the reference vector $\vec{m}$ can be expressed as:

$$\vec{m} = \frac{p_1}{l_1} \vec{v}_1 + \frac{p_2}{l_2} \vec{v}_2 + \left(1 - \frac{p_1}{l_1} - \frac{p_2}{l_2}\right) \vec{v}_3 . \tag{3.18}$$

From (3.18), the duty cycles of the vectors can be directly deduced as follows:

$$d_1 = \frac{p_1}{l_1}, \quad d_2 = \frac{p_2}{l_2}, \quad \text{and} \quad d_3 = 1 - \frac{p_1}{l_1} - \frac{p_2}{l_2} . \tag{3.19}$$

If the balanced SV diagram is normalized to have triangular regions with unity lengths ($l_1 = l_2 = 1$), the calculation of those duty cycles is simplified as:

$$d_1 = p_1, \quad d_2 = p_2, \quad \text{and} \quad d_3 = 1 - p_1 - p_2 . \tag{3.20}$$

Calculation of duty cycles using this method is actually very functional. However, the former condition that all the areas must be equilateral triangles is only possible if the voltages of the DC-link capacitors are balanced. Thus, when dealing with the unbalanced case (Chapter 5), these lengths can no longer be considered to be unity because they change according to the present imbalance. In that case, (3.19) must be applied.

3.2. The Three-Level Converter

3.2.1. SVM Under Voltage-Balanced Conditions

Suitable vectors from the SV diagram should be chosen for each modulation cycle in order to generate the reference vector ($\vec{m}$). The vectors nearest to $\vec{m}$ are the most appropriate selections in terms of their ability to minimize the switching frequencies of the power devices, improve the quality of the output voltage spectra, and the electromagnetic interference (EMI).

In Fig. 3.9, the SV diagram of the three-level converter is divided into sextants, and each sextant is then divided into four triangular regions in order to show the vectors nearest to the reference.

***Fig. 3.9.** Three-level vector diagram divided into sextants and regions*.

Four groups of vectors can be distinguished in this diagram, as described in the following.

(1) The "large vectors" (200, 220, 020, 022, 002 and 202) assign the output voltages of the converter to either the highest or the lowest DC voltage levels. As they do not connect any output to the NP, they do not affect the voltage balance of the capacitors. These vectors can generate the highest AC voltage amplitudes

because they have the greatest lengths. In fact, these six vectors are equivalent to the active ones of the two-level converter.

(2) The "medium vectors" (210, 120, 021, 012, 102 and 201) connect each output to a different DC-link voltage level. Under balanced conditions, their tip end in the middle of the segments that join two consecutive large vectors. The length of the medium vectors defines the maximum amplitude of the reference vector for linear modulation and steady-state conditions, which is $\sqrt{3}/2$ the length of the large vectors. Since one output is always connected to the NP, the corresponding output current will define the NP current (i_1). This connection produces voltage imbalances in the capacitors, and these must be compensated.

(3) The "short vectors" (100-211, 110-221, 010-121, 011-122, 001-112 and 101-212) connect the AC outputs to two consecutive DC-link voltage levels. Their length is half the length of the large vectors. They are double vectors, which means that two states of the converter can generate the same voltage vector. As they affect the NP current in opposite ways, proper utilization of these vectors will help the NP voltage to achieve balance.

(4) The "zero vectors" (000, 111 and 222) are in the origin of the diagram. They connect all of the outputs of the converter to the same DC-link voltage level, and therefore, they do not produce any current in the DC side.

3.2.2. Simplified Calculation of Duty Cycles

Taking into account the symmetry of all the sextants, it is interesting to reflect the reference vector into the first sextant in order to reduce the number of relevant regions (Appendix B). Also, the amplitude of the reference vector must be normalized to fit into a diagram in which the triangular regions have unity lengths.

The theoretical maximum length of the normalized reference vector ($\vec{m}_n$) is the two-unity value. However, in steady-state conditions, its length is limited to $\sqrt{3}$ due to the fact that longer lengths of this vector will be outside of the vector-diagram hexagon (Fig. 3.10), and thus cannot be generated by modulation. Overmodulation is produced if the normalized reference vector assumes lengths longer than $\sqrt{3}$ for some positions of this vector, but it can never be outside of the hexagon (overmodulation is covered in Section 6.5.)
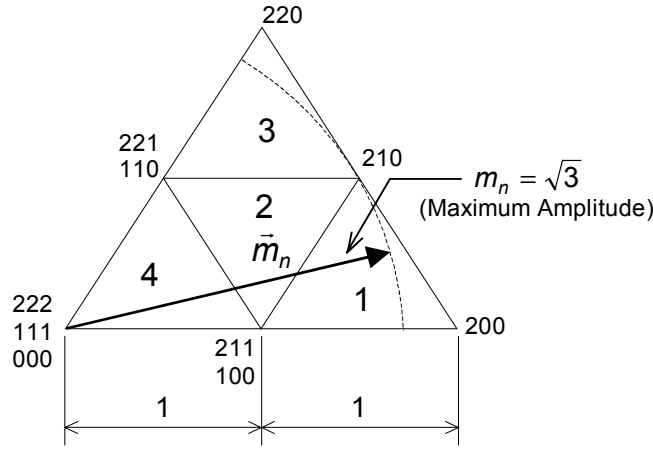
Fig. 3.10. *Maximum length of the normalized reference vector in steady-state conditions.*

Defining a modulation index m that potentially uses values in the interval $m \in [0, 1]$ for linear modulation, the length of the normalized reference vector would be:

$$m_n = \sqrt{3}\, m \qquad \left(0 \le m_n \le \sqrt{3} \right). \tag{3.21}$$

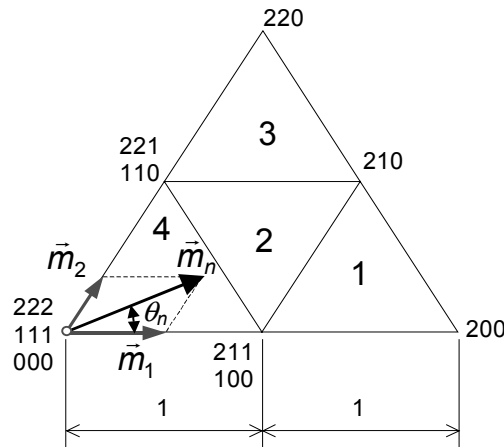In Fig. 3.11, the normalized reference vector is decomposed into the axes located at zero and sixty degrees, obtaining projections m_1 and m_2, respectively.

Fig. 3.11. *Projections of the normalized reference vector in the first sextant.*

The lengths of the new vectors are determined as follows:

$$m_1 = m_n \left(cos\,\theta_n - \frac{sin\,\theta_n}{\sqrt{3}} \right) \qquad \text{and} \qquad m_2 = 2m_n \frac{sin\,\theta_n}{\sqrt{3}}. \tag{3.22}$$

In accordance with the general method revealed in Section 3.1.5, these values are the direct duty ratios of the vectors, as in the following:

$$d_{100\,/\,211} = m_1, \quad d_{110\,/\,221} = m_2 \quad \text{and} \quad d_{111} = 1 - m_1 - m_2. \tag{3.23}$$

Even though there are three redundant vectors in the origin, only the combination "111" is considered because it achieves the best modulation sequences in terms of switching frequency.

The cases for which the normalized reference vector is located in Regions 1, 2 and 3 are shown in Fig. 3.12.
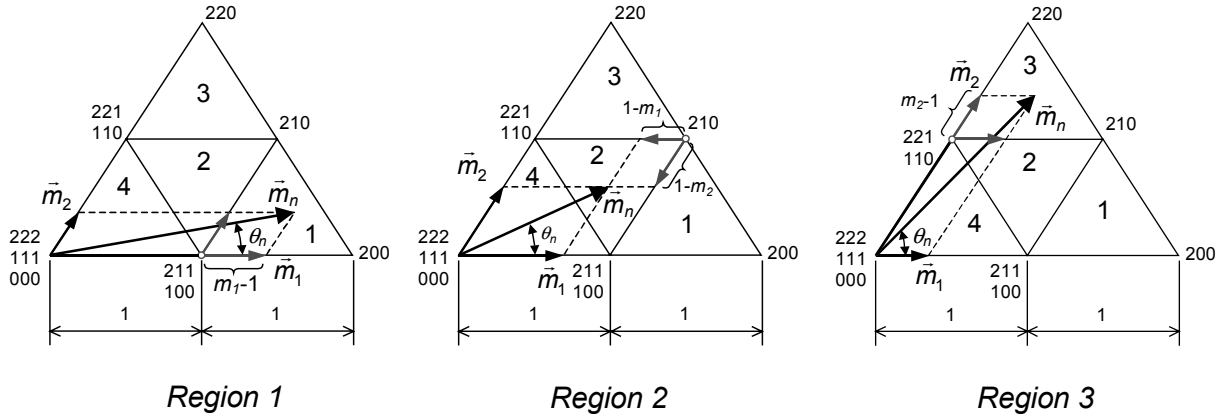

Region 1   *Region 2*   *Region 3*

Fig. 3.12. *Projections for Regions 1, 2 and 3.*

Table 3.1 summarizes the information needed to ascertain the region where the reference vector lies and the duty cycles of the nearest vectors in the first sextant.

Table 3.1. *Summary of information for the SVM.*

Case	Region	Duty Cycles
$m_1 > 1$	1	$d_{200} = m_1 - 1$ $d_{210} = m_2$ $d_{100/211} = 2 - m_1 - m_2$
$m_1 \leq 1$ $m_2 \leq 1$ $m_1 + m_2 > 1$	2	$d_{100/211} = 1 - m_2$ $d_{110/221} = 1 - m_1$ $d_{210} = m_1 + m_2 - 1$
$m_2 > 1$	3	$d_{210} = m_1$ $d_{220} = m_2 - 1$ $d_{110/221} = 2 - m_1 - m_2$
$m_1 \leq 1$ $m_2 \leq 1$ $m_1 + m_2 \leq 1$	4	$d_{100/211} = m_1$ $d_{110/221} = m_2$ $d_{111} = 1 - m_1 - m_2$

For all cases, it is assumed that the sum of m_1 and m_2 is not greater than 2; otherwise, the reference vector would be outside of the hexagon, and thus could not be reproduced by modulation.

3.2.3. The dq-gh Transformation

It is quite common for the control stage to provide the reference vector in terms of dq coordinates. Transformation (3.24) is proposed to translate these dq components directly into some very useful variables for the modulation:

$$\begin{bmatrix} m_g \\ m_h \end{bmatrix} = \mathbf{T}_{dq-gh} \begin{bmatrix} m_d \\ m_q \end{bmatrix} \quad \text{with} \tag{3.24}$$

$$\mathbf{T}_{dq-gh} = k \frac{\sqrt{2}}{V_{DC}/(n-1)} \begin{bmatrix} \sin(\theta_r + 2\pi/3) & \cos(\theta_r + 2\pi/3) \\ \sin\theta_r & \cos\theta_r \end{bmatrix},$$

where θ_r is the coordinate reference angle.

Using this transformation, the control signals given in the orthogonal rotating coordinate frame (the dq components) are directly translated into a non-orthogonal base in the stationary coordinate frame (as gh components). In fact, the new reference axes are the ones that limit the first sextant, and which are separated by 60º.

Fig. 3.13. *Graphical representation of the dq-gh transformation.*

The value of the coefficient *k* in (3.24) must be defined so that in the new axes, the SV diagram will fit into a two-unit-per-side hexagon. This coefficient depends on which sort of variables (phase or line-to-line variables) are processed for the control, and also on the coefficient used for the dq transformation. For example, when using a power-conservative dq transformation (coefficient $\sqrt{2/3}$) and dealing with phase variables, the parameter *k* must be unity. When the line-to-line variables are used for the control, *k* must be $1/\sqrt{3}$.

From the values m_g and m_h, the sextant where the reference vector lies can be directly found, as can the components m_1 and m_2 of the equivalent vector in the first sextant (Appendix B). These relationships are illustrated in Fig. 3.14 and Table 3.2.
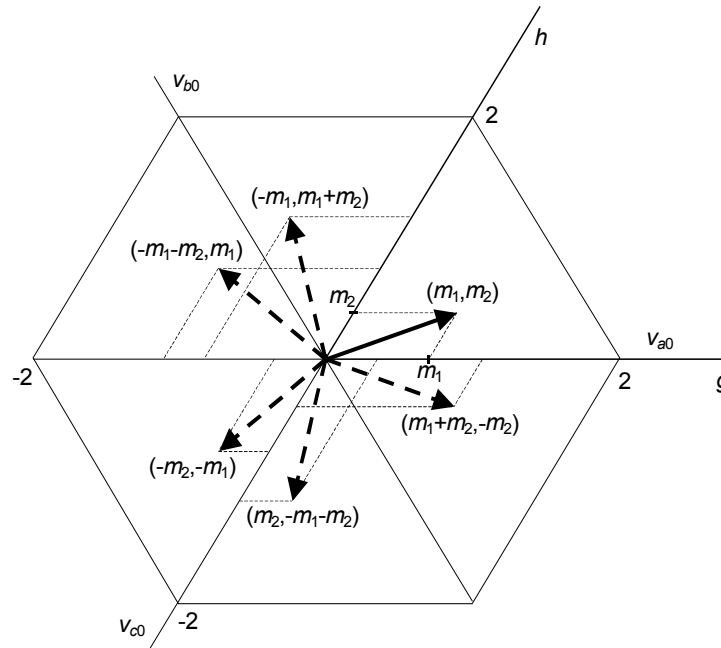
Fig. 3.14. *Components gh from different reference vectors. Equivalences in the first sextant*.

Table 3.2. *Determination of the sextant and the equivalent components m_1 and m_2 in the first sextant.*

gh Components (m_g, m_h)			Sextant	Equivalent Components in the First Sextant (m_1, m_2)	
$m_g{\geq}0$	$m_h{\geq}0$		1st	$m_1=m_g$	$m_2=m_h$
$m_g{<}0$	$m_h{\geq}0$	$m_g+m_h{\geq}0$	2nd	$m_1=-m_g$	$m_2=m_g+m_h$
$m_g{<}0$	$m_h{\geq}0$	$m_g+m_h{<}0$	3rd	$m_1=m_h$	$m_2=-m_g-m_h$
$m_g{<}0$	$m_h{<}0$		4th	$m_1=-m_h$	$m_2=-m_g$
$m_g{\geq}0$	$m_h{<}0$	$m_g+m_h{<}0$	5th	$m_1=-m_g-m_h$	$m_2=m_g$
$m_g{\geq}0$	$m_h{<}0$	$m_g+m_h{\geq}0$	6th	$m_1=m_g+m_h$	$m_2=-m_h$

Using a DSP to process the duty cycles of the vectors will be very fast if the dq-gh transformation is applied and Tables 3.1 and 3.2 are used.

3.2.4. Defining Real Vectors

When the most suitable sequence for the vectors in the first sextant to achieve low switching frequency has been defined, the next and final step is to apply the calculated duty cycles to the corresponding vectors. This task requires the knowledge of the real sextant in which the reference vector lies (Table 3.2), and it can be performed by simply interchanging the states of the output phases in accordance with the equivalences given in Table 3.3. The sequences of vectors obtained in the corresponding sextant will preserve the same switching frequencies that the original sequence defined in the first sextant.

Table 3.3. Interchanges of the output states depending on the sextant in which the reference vector lies (after making calculations in the first sextant).

1st Sextant	2nd Sextant	3rd Sextant	4th Sextant	5th Sextant	6th Sextant
a	$a \to b$	$a \to b$	$a \to c$	$a \to c$	a
b	$b \to a$	$b \to c$	b	$b \to a$	$b \to c$
c	c	$c \to a$	$c \to a$	$c \to b$	$c \to b$

3.2.5. Modulation Techniques

So far, the duty cycles of the vectors nearest to the reference have been calculated. However, the short vectors used in each modulation period are not yet defined. Two techniques are discussed in this dissertation: NTV modulation and symmetric modulation.

3.2.5.1. NTV Modulation

The NTV modulation technique uses only three of the closest vectors per modulation cycle. Thus, a single short vector will be selected from each pair. The choice is made according to the objective of maintaining balanced voltages in the DC-link capacitors; therefore, the present voltage imbalance and the direction of the instantaneous output currents must be known. The NP current (i_1) must be positive in order to discharge the lower capacitor, and must be negative to charge it. For example, if i_a is positive, vector 100 will discharge the lower capacitor ($i_1=i_a>0$), and vector 211 will charge it ($i_1=i_b+i_c= -i_a<0$).
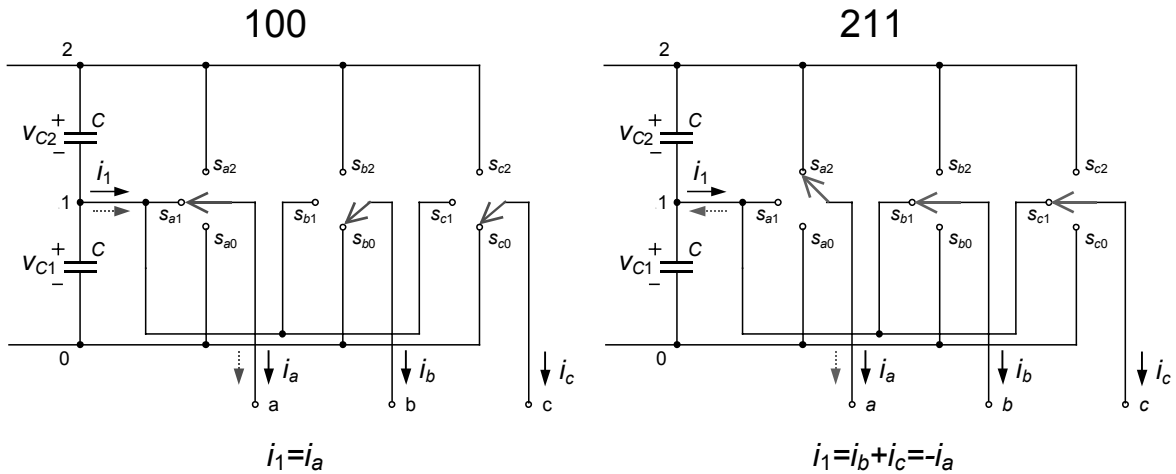
Fig. 3.15. *Example of control of the NP current by proper selection of the double vectors.*
Vector 100 produces $i_1=i_a$, whereas vector 211 produces $i_1=i_b+i_c=-i_a$.

Since all of the modulation will be calculated in the first sextant, this criterion can be expressed as shown in Table 3.4(a). When the reference vector lies in the first sextant, currents $i_a{}'$ and $i_c{}'$ in these tables will be i_a and i_c, respectively, but they must be changed when it lies in another sextant. These equivalences are given in Table 3.4(b).

Table 3.4. *(a) Criteria for selection between vectors 100 and 211, and vectors 110 and 221; and (b) equivalences of currents to process calculations in the first sextant.*

(a)

Selection between 100 and 211			Selection between 110 and 221		
$v_{C1}>v_{C2}$	$i_a{}'>0$	y_1	$v_{C1}>v_{C2}$	$i_c{}'>0$	y_2
0	0	0 (100)	0	0	1 (221)
0	1	1 (211)	0	1	0 (110)
1	0	1 (211)	1	0	0 (110)
1	1	0 (100)	1	1	1 (221)

$$y_1 = (v_{C1} > v_{C2}) \oplus (i_a{}' > 0) \qquad y_2 = \overline{(v_{C1} > v_{C2}) \oplus (i_c{}' > 0)}$$

(b)

Equivalences	1st Sext.	2nd Sext.	3rd Sext.	4th Sext.	5th Sext.	6th Sext.
$i_a{}'$	i_a	i_b	i_b	i_c	i_c	i_a
$i_c{}'$	i_c	i_c	i_a	i_a	i_b	i_b

Table 3.5 shows the sequences of the vectors in the first sextant that are more capable of minimizing the switching frequencies of the devices. These sequences depend on the short vectors that are selected according to voltage-balance requirements. The number of changes or steps between consecutive vectors

associated with each sequence is also indicated in this table. The worst cases are Region 2 (vectors 100-221) and Region 4 (vectors 100-221), both of which require four switching steps, which is twice the number required by any other sequences. When a sequence is repeated in a subsequent modulation period, the sequence is flipped in order to minimize the number of steps from one cycle to the next.

Table 3.5. Sequences of vectors in the first sextant by NTV modulation.

Region	Short Vectors	Sequences	Steps
1	100	100-200-210 // 210-200-100	2 // 2
1	211	200-210-211 // 211-210-200	2 // 2
2	100-110	100-110-210 // 210-110-100	2 // 2
2	100-221	100-210-221 // 221-210-100	4 // 4
2	211-110	110-210-211 // 211-210-110	2 // 2
2	211-221	210-211-221 // 221-211-210	2 // 2
3	110	110-210-220 // 220-210-110	2 // 2
3	221	210-220-221 // 221-220-210	2 // 2
4	100-110	100-110-111 // 111-110-100	2 // 2
4	100-221	100-111-221 // 221-111-100	4 // 4
4	211-110	110-111-211 // 211-111-110	2 // 2
4	211-221	111-211-221 // 221-211-111	2 // 2

Since the selection of the double vectors in the NTV modulation is based on comparators and logical functions, a nonlinear control is performed. Although it is not possible to achieve a value that is precisely zero for the average NP current over a modulation period, if the short vectors are properly chosen, the sign of this average current tends to balance those voltages, and the objective is nonetheless generally achieved (this is not true for all cases, as discussed in Section 3.2.6.1).

Despite the simplicity of using only three vectors per modulation cycle, the following drawbacks exist:

-    there are significant switching-frequency ripples in the voltages of the capacitors; and

-    when changing sequences due to a new region or different selection of short vectors, two switching steps can be produced (two legs must switch one level). Due to this fact, and that there are some sequences that require four steps (Table 3.5), the switching frequencies will not be constant.

The symmetric modulation approach can overcome these disadvantages and keep constant the switching frequency.

3.2.5.2. Symmetric Modulation

Symmetric modulation is characterized by using four vectors per modulation sequence. Dealing with another variable in the calculation of the duty cycles allows the equation of the NP current to be included in the equation system:

$$\vec{m} = d_1\vec{v}_1 + d_2\vec{v}_2 + d_3\vec{v}_3 + d_4\vec{v}_4 , \qquad (3.25a)$$

$$d_1 + d_2 + d_3 + d_4 = 1, \text{ and} \qquad (3.25b)$$

$$\bar{i}_1 = \sum_{i,j,k \in \{0,2\}} \left[(d_{1jk} - d_{i11}) i_a + (d_{i1k} - d_{1j1}) i_b + (d_{ij1} - d_{11k}) i_c \right] = 0 . \qquad (3.25c)$$

Equation (3.25a) is, in fact, a pair of equations. Equation (3.25c) shows the relationship between the local averaged value of the NP current, the duty cycles of the vectors, and the AC currents. Mathematically speaking, this new equation allows the NP current to equal zero each modulation period.

Symmetric modulation is very similar to NTV in some respects. The new vector added to the sequence is one of the short vectors that was not selected using NTV. Thanks to this, the duty cycles are basically calculated by the same process, with the only difference being that the duty cycle applied in NTV to only one of the dual vectors is now shared between both of them. For instance, if the reference vector lies in Region 1, the sequence will be 100-200-210-211. To satisfy the zero-NP-current condition, the duty cycle calculated for 100/211 should now be properly distributed between them.
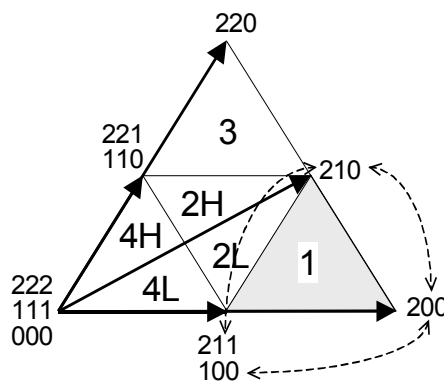
Fig. 3.16. *New regions for symmetric modulation. Example of vector sequence for Region 1.*
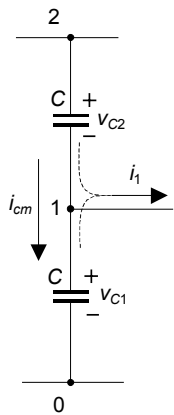
For this modulation, Regions 2 and 4 are now split into 2L, 2H, 4L and 4H. The line that divides such regions, which coincides with vector 210, has been drawn according to a geometric-symmetry criterion. The best vector sequences in the first

sextant are given in Table 3.6; these sequences best minimize the switching frequencies of the devices.

Table 3.6. *Sequences of vectors in the first sextant by symmetric modulation.*

Regions	Sequences	Steps
1	100-200-210-211 // 211-210-200-100	3 // 3
2L	100-110-210-211 // 211-210-110-100	3 // 3
2H	110-210-211-221 // 221-211-210-110	3 // 3
3	110-210-220-221 // 221-220-210-110	3 // 3
4L	100-110-111-211 // 211-111-110-100	3 // 3
4H	110-111-211-221 // 221-211-111-110	3 // 3

In general terms, the local averaged NP current must be zero to achieve constant voltage in the NP. However, the exact NP current required must be calculated for each modulation period in order to compensate for errors that occur due to tolerances and some assumptions. A modulation period delay is taken into account to obtain the reference NP current, so that the value calculated during the present period will be applied the next one. The voltages of the capacitors at the beginning of the next period (*k*+1) are:

$$
\begin{cases}
v_{C2(k+1)} = \dfrac{1}{C} \displaystyle\int_{kT_m}^{(k+1)T_m} \left(i_{cm} + i_1/2\right)dt + v_{C2(k)}, \text{ and} \\[4mm]
v_{C1(k+1)} = \dfrac{1}{C} \displaystyle\int_{kT_m}^{(k+1)T_m} \left(i_{cm} - i_1/2\right)dt + v_{C1(k)}.
\end{cases}
\tag{3.26}
$$

The component i_{cm} in (3.26) is the common current through both DC-link capacitors. On the other hand, the NP current (i_1) splits into 50% for each capacitor according to the general expression given in (4.4).

These voltages at the end of the next period can be expressed as:

$$
\begin{cases}
v_{C2(k+2)} = \dfrac{1}{C} \displaystyle\int_{(k+1)T_m}^{(k+2)T_m} \left(i_{cm} + i_1/2\right)dt + v_{C2(k+1)}, \text{ and} \\[4mm]
v_{C1(k+2)} = \dfrac{1}{C} \displaystyle\int_{(k+1)T_m}^{(k+2)T_m} \left(i_{cm} - i_1/2\right)dt + v_{C1(k+1)}.
\end{cases}
\tag{3.27}
$$

Substituting (3.26) into (3.27) and imposing the balance condition $v_{C2}(k+2) = v_{C1}(k+2)$ reveals that

$$v_{C2}(k) = -\frac{1}{C}\int_{(k+1)T_m}^{(k+2)T_m} i_1\, dt - \frac{1}{C}\int_{kT_m}^{(k+1)T_m} i_1\, dt + v_{C1}(k).$$ (3.28)

The common current i_{cm} has disappeared in (3.28) because this current does not affect the NP voltage balance. Finally, this equation can be rewritten as:

$$\bar{i}_1(k+1) = \frac{C}{T_m}\left[v_{C1}(k) - v_{C2}(k)\right] - \bar{i}_1(k),$$ (3.29)

where $\bar{i}_1(k+1)$ and $\bar{i}_1(k)$ are the discrete local averaged values of i_1 over each respective modulation period, such that

$$\bar{i}_1(k) = \frac{1}{T_m}\int_{kT_m}^{(k+1)T_m} i_1\, dt, \quad \text{and} \quad \bar{i}_1(k+1) = \frac{1}{T_m}\int_{(k+1)T_m}^{(k+2)T_m} i_1\, dt.$$ (3.30)

Therefore, (3.29) defines the averaged NP current required to achieve voltage balance in the capacitors at the end of the next modulation period. Notice that all the voltages in this equation are sensed at the beginning of the present period k.
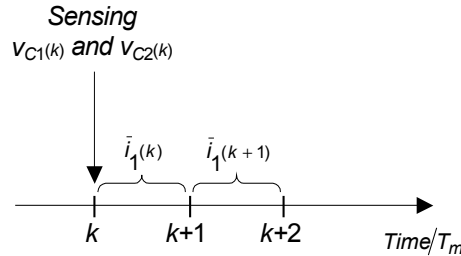
Fig. 3.17. Sequence of modulation cycles.

Since the local averaged NP current reference $\bar{i}_1(k+1)$ is given by (3.29), the next step is to achieve this value by properly distributing the duty cycle of the short vectors. The instantaneous NP current i_1 can be expressed in terms of the control functions of these vectors as:

$$i_1 = -(s_{211} - s_{100})i_a + s_{210}i_b + (s_{221} - s_{110})i_c.$$ (3.31)

Assuming constant AC output currents during a modulation period, the discrete local averaged operator transforms this expression into:

$$\bar{i}_1(k) = -[d_{211}(k) - d_{100}(k)]i_a(k) + d_{210}(k)i_b(k) + [d_{221}(k) - d_{110}(k)]i_c(k).$$ (3.32)

For the next modulation period $k+1$

$$\bar{i}_{1(k+1)} = -\left[d_{211(k+1)} - d_{100(k+1)}\right] i_{a(k+1)} + d_{210(k+1)} i_{b(k+1)} + $$
$$+ \left[d_{221(k+1)} - d_{110(k+1)}\right] i_{c(k+1)}. \tag{3.33}$$

Two cases can be distinguished depending on the position of the reference vector. If the tip of the reference vector lies in Regions 1, 2L or 4L ($\theta_n \leq 30°$ or $m_1 \geq m_2$), vectors 100-211 define the beginning and ending of each modulation sequence. These vectors can be distributed according to a variable x_1:

$$d_{100} = \frac{d_{100/211}}{2}(1 - x_1), \quad \text{and} \quad d_{211} = \frac{d_{100/211}}{2}(1 + x_1). \tag{3.34}$$

Since the duty cycles must be positive, this distribution variable considers values in the interval $x_1 \in \left[-1, 1\right]$. Taking into account the vectors used in these regions, $\bar{i}_{1(k+1)}$ can be expressed as:

$$\bar{i}_{1(k+1)} = -d_{100/211(k+1)} x_{1(k+1)} i_{a(k+1)} + d_{210(k+1)} i_{b(k+1)} - d_{110(k+1)} i_{c(k+1)}. \tag{3.35}$$

Isolating the variable $x_{1(k+1)}$ obtains the following:

$$x_{1(k+1)} = \frac{d_{210(k+1)} i_{b(k+1)} - d_{110(k+1)} i_{c(k+1)} - \bar{i}_{1(k+1)}}{d_{100/211(k+1)} i_{a(k+1)}}. \tag{3.36}$$

Due to the intrinsic delay of the modulation process, most of the variables in (3.36) are known during the present period k. The duty cycles are calculated during this k period, and the value of $\bar{i}_{1(k+1)}$ is the exact averaged current required to reach voltage balance, as defined by (3.29). However, the AC currents during the next period $k+1$ are unknown, since they are sensed at the beginning of the period k. Yet, these currents can be extrapolated to the next period by using the first-order Taylor's Series, as follows:

$$i_{a,b,c(k+1)} \approx i_{a,b,c(k)} + \frac{i_{a,b,c(k)} - i_{a,b,c(k-1)}}{T_m} T_m = 2i_{a,b,c(k)} - i_{a,b,c(k-1)} \tag{3.37}$$

On the other hand, if the reference vector lies in Regions 3, 2H or 4H ($\theta_n > 30°$ or $m_1 < m_2$), vectors 110-221 will be the beginnings and endings of all of the modulation sequences. Similarly, the distribution variable x_2 can be calculated as

$$x_{2(k+1)} = \frac{d_{211(k+1)} i_{a(k+1)} - d_{210(k+1)} i_{b(k+1)} + \bar{i}_{1(k+1)}}{d_{110/221(k+1)} i_{c(k+1)}}, \tag{3.38}$$

and the duty cycles of vectors 110 and 221 will be

$$d_{110} = \frac{d_{110/221}}{2}(1 - x_2), \quad \text{and} \quad d_{221} = \frac{d_{110/221}}{2}(1 + x_2), \quad (3.39)$$

where $x_2 \in \left[-1, 1\right]$.

If the distribution variables x_1 and x_2 have values outside the interval $\left[-1, 1\right]$, they remain saturated to the closest limit.

Equations (3.36) and (3.38) provide the values of the distribution variables in the first sextant. If the reference vector is not in this sextant, the AC currents will be interchanged according to the real sextant. These equivalences are given in Table 3.7.

Table. 3.7. Equivalences of currents.

1st Sextant	2nd Sextant	3rd Sextant	4th Sextant	5th Sextant	6th Sextant
i_a	$i_a \rightarrow i_b$	$i_a \rightarrow i_b$	$i_a \rightarrow i_c$	$i_a \rightarrow i_c$	i_a
i_b	$i_b \rightarrow i_a$	$i_b \rightarrow i_c$	i_b	$i_b \rightarrow i_a$	$i_b \rightarrow i_c$
i_c	i_c	$i_c \rightarrow i_a$	$i_c \rightarrow i_a$	$i_c \rightarrow i_b$	$i_c \rightarrow i_b$

3.2.5.3. Simulated Results

NTV and symmetric modulation are tested by simulation in the following. For all of the examples, the converter is supplied by a DC voltage source V_{DC}=1800 V and operates with an R-L star-connected load with parameters R=1 Ω and L=2 mH. The DC-link capacitors are C=1000 μF and the fundamental frequency of the AC voltages is f=50 Hz. Both modulation techniques have been checked for different modulation indices (m) and modulation periods (T_m).

The values of the total harmonic distortion (THD) given in the figures consider the following definition:

$$THD(\%) = 100 \frac{\sqrt{\sum_{h=2}^{\infty} \hat{V}_h^2}}{\hat{V}_1}, \quad (3.40)$$

in which $\hat{V}_h$ is the amplitude of the h-order harmonic. This expression can be better handled with the following simplification:

$$THD(\%) = 100\sqrt{\frac{\sum\limits_{h=1}^{\infty} \hat{V}_h^2}{\hat{V}_1^2} - 1} = 100\sqrt{\frac{2V_{RMS}^2}{\hat{V}_1^2} - 1} \qquad (3.41)$$

in which V_{RMS} is the RMS value of the waveform.

Fig. 3.18 and Fig. 3.19 show the voltages of the DC-link capacitors (v_{C1} and v_{C2}), a line-to-line voltage (v_{ab}) and the output currents (i_a, i_b and i_c) when the converter operates with modulation period T_m= 50 μs (or modulation frequency f_m=20 kHz). NTV is tested in Fig. 3.18 and symmetric modulation in Fig. 3.19.

Symmetric modulation generates better output voltage spectra, since the first group of harmonics have frequencies around half of the modulation frequency, while the spectra of the NTV contain lower frequency components. Additionally, symmetric modulation generates less THD. Another advantage is the smaller amplitude of the high-frequency ripple in the voltages of the capacitors. Nevertheless, two important disadvantages of symmetric modulation must be remarked on. On the one hand, there exists a low-frequency ripple in the voltages of the capacitors when the converter operates with low modulation indices. This fact is a consequence of the lesser degree of freedom in the utilization of redundant vectors, since one of the dual vectors cannot be chosen in regions 2L, 2H, 4L and 4H. On the other hand, the switching frequencies of the devices are higher with symmetric modulation. The mean switching frequencies ($f_{s\,mean}$) given in the figures are calculated for complete turn-on and turn-off cycles in all the switches of the bridge and divided by 12.

In Fig. 3.20 the converter operates with a modulation period of T_m= 500 μs (or modulation frequency f_m=2 kHz). NTV is tested under two conditions, the "normal" NTV presented in Fig. 3.20(a), which does not consider the intrinsic one-period delay that exists between sensing variables and application of the modulation, and the NTV shown in Fig. 3.20(b), in which the values of the sensed voltages and currents are extrapolated to the next modulation period. In the second case, less NP voltage ripple is achieved but at the price of higher switching frequencies of the devices.

Symmetric modulation is applied in Fig. 3.20(c). In accordance with Section 3.2.5.2, this modulation includes compensation for one-period delay. Since the objective of this modulation is to achieve equal voltages in the capacitors at the end of any modulation period, the NP voltage ripple produced by the switching frequency has less amplitude. A magnified detail of these voltages is presented in Fig. 3.21.
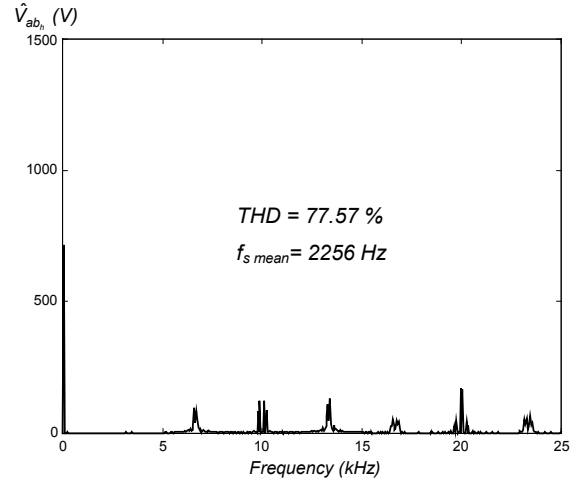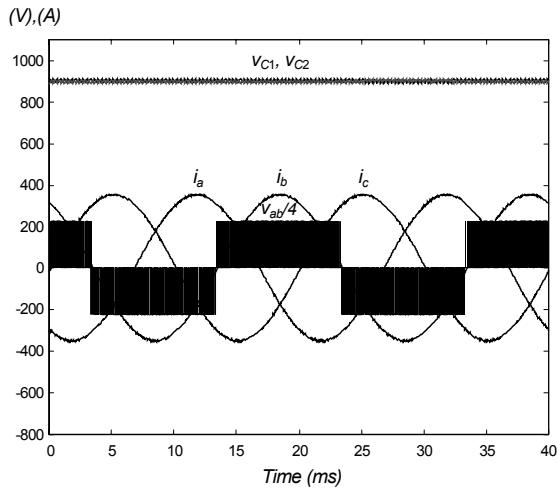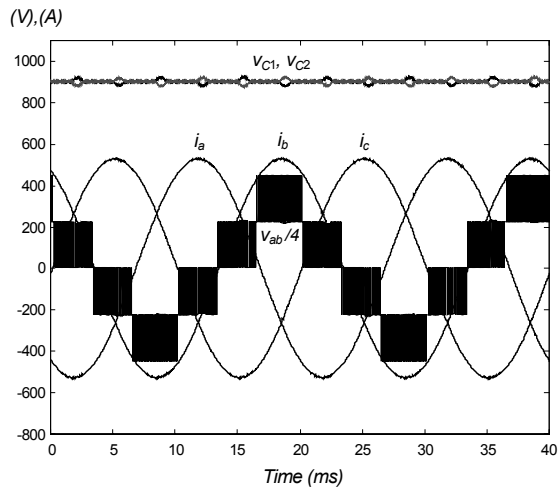
(a)
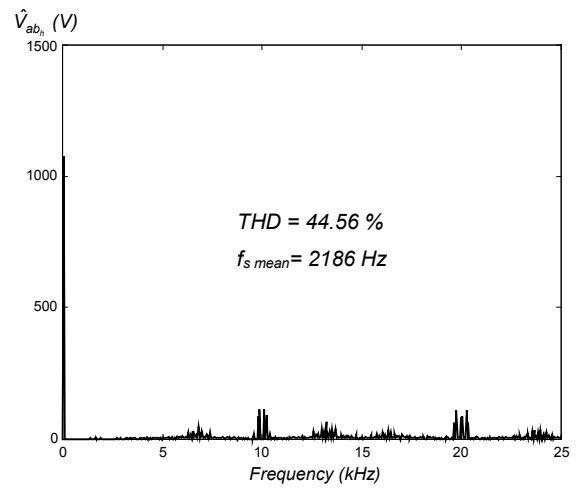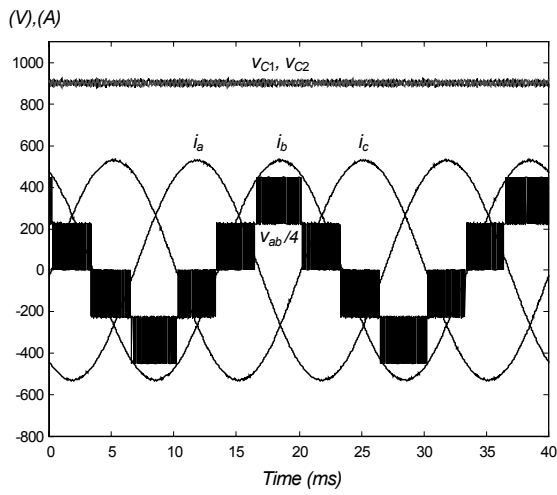
(b)
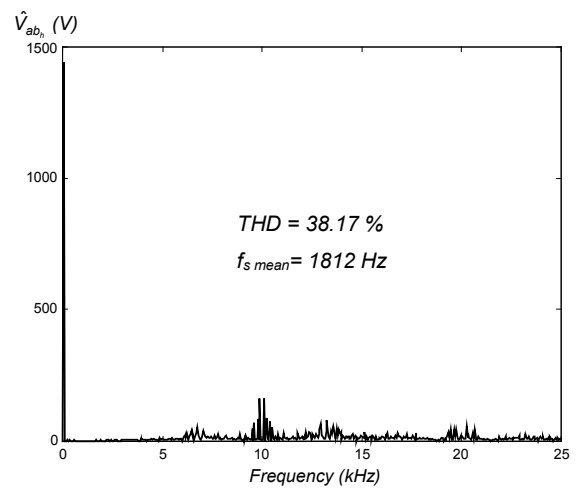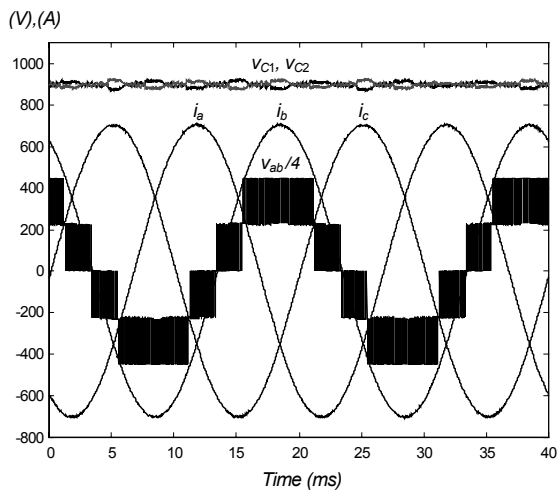
(c)

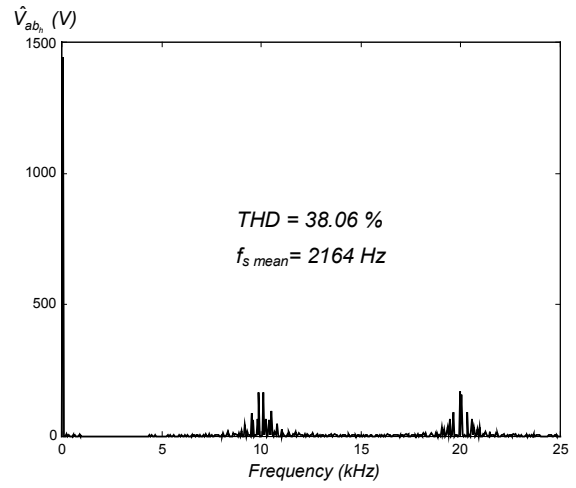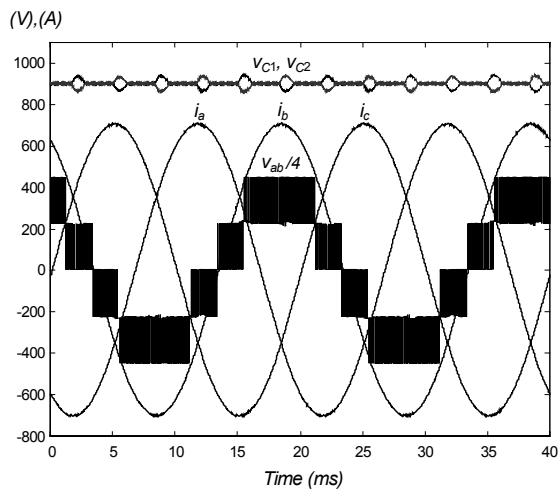**Fig. 3.18.** *NTV modulation with modulation period T_m=50 μs:*
(a) m=0.4; (b) m=0.6; and (c) m=0.8.
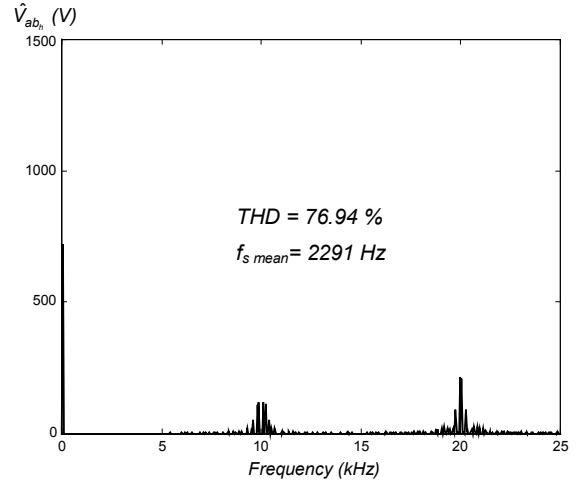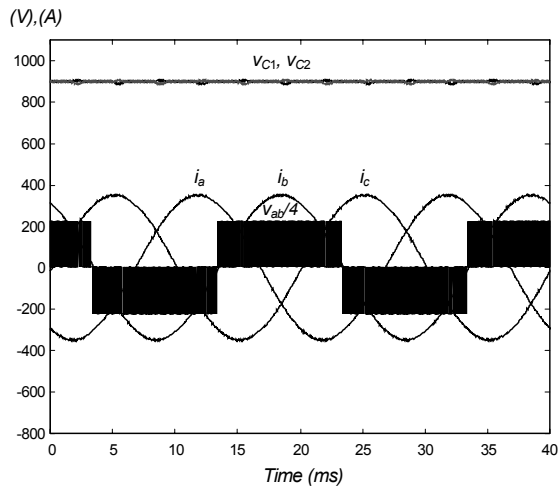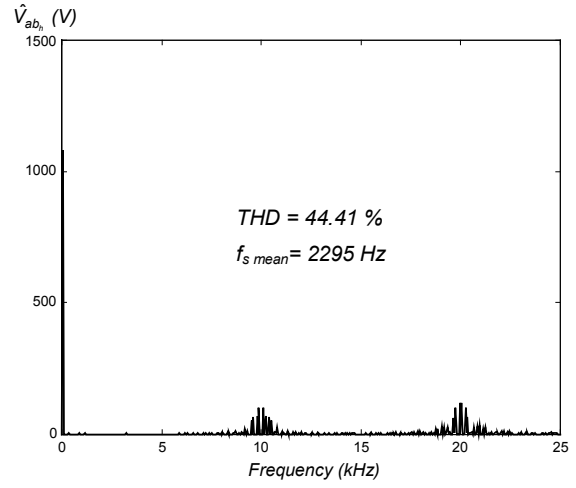
Fig. 3.19. *Symmetric modulation with modulation period T_m=50 μs:*
(a) m=0.4; (b) m=0.6; and (c) m=0.8.
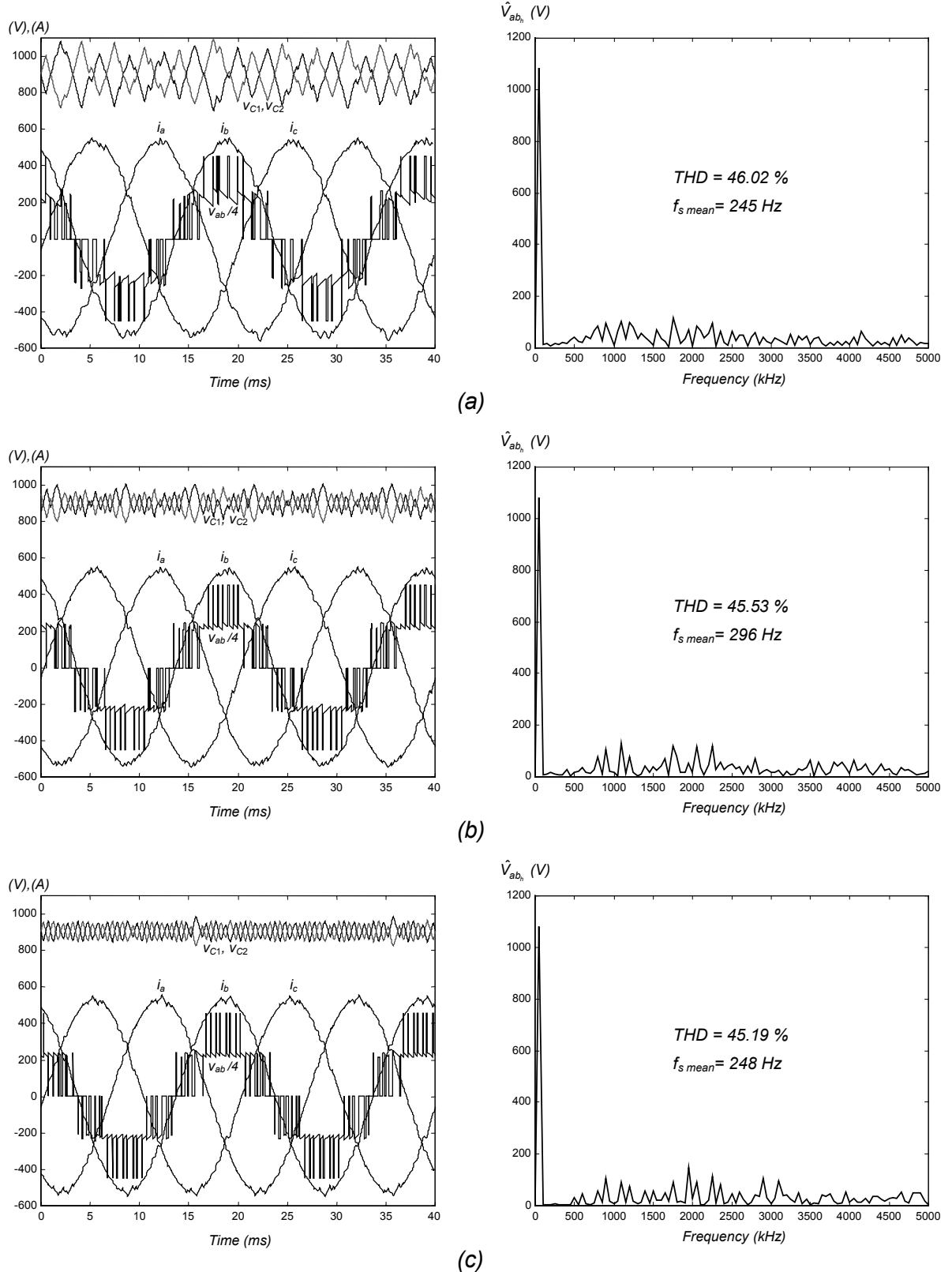
(a)

(b)

(c)

Fig. 3.20. *NTV and symmetric modulation with modulation period T_m=500 μs and m=0.6: (a) NTV; (b) NTV with compensation for one-period delay; and (c) symmetric modulation.*
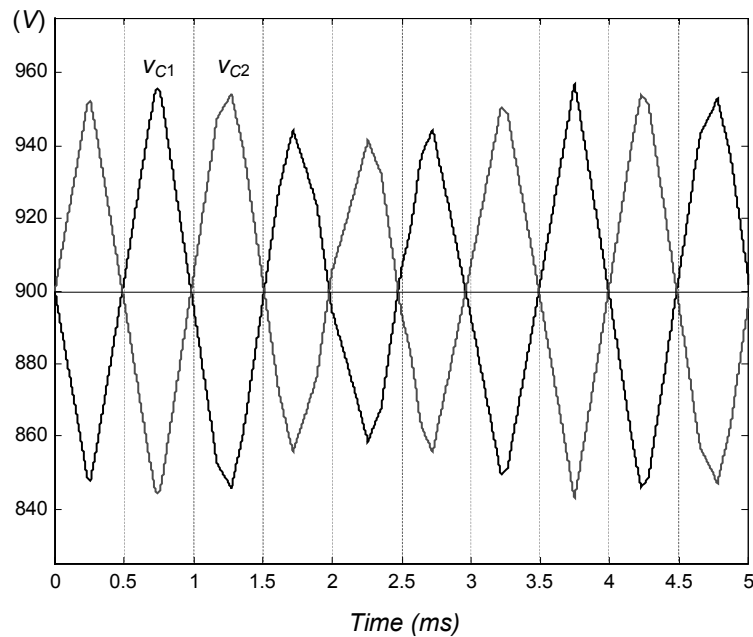
Fig. 3.21. *Voltages in the DC-link capacitors with symmetric modulation. Magnification from Fig. 3.20(c).*

In conclusion, NTV presents some interesting advantages when the converter operates with small modulation periods. These advantages are the greater control of the low-frequency NP voltage ripple, the lower switching frequencies in the devices, as well as the easier implementation because of fewer calculations required for NP voltage control. Symmetric modulation presents advantage when the converter operates with large modulation periods. In such conditions, the NP voltage ripple produced by the switching frequency becomes significant and this modulation technique can handle it better than NTV.

3.2.6. Limits of Control of the Voltage Balance

In this section, the limits of the ability to control the NP balance for both modulation techniques are revealed.

When the reference vector is located in the first sextant, the local averaged NP current can be expressed as:

$$\bar{i}_1 = \mathbf{D}\, \mathbf{i}_{ph}, \tag{3.40}$$

$$\text{with} \quad \mathbf{D} = \left[(d_{100} - d_{211}) \quad d_{210} \quad (d_{221} - d_{110}) \right]$$

$$\text{and} \quad \mathbf{i}_{ph} = \left[i_a \quad i_b \quad i_c \right]^{\mathsf{T}}.$$

To validate this expression for the entire vector diagram, the equivalent AC currents for each sextant must be taken into account. This correction should be done according to Table 3.7.

A new transformation matrix $\mathbf{S}$ is introduced for the purpose of interchanging the currents depending on which sextant the reference vector occupies, as follows:

$$\bar{i}_1 = \mathbf{D}\, \mathbf{S}\, \mathbf{i}_{ph}, \quad \text{with} \quad \mathbf{S} = \begin{bmatrix} s_1 + s_6 & s_2 + s_3 & s_4 + s_5 \\ s_2 + s_5 & s_1 + s_4 & s_3 + s_6 \\ s_3 + s_4 & s_5 + s_6 & s_1 + s_2 \end{bmatrix}, \tag{3.41}$$

where s_i defines the sextant in which the reference vector lies, such that

$$s_i = \begin{cases} 1 & \text{if } \vec{m} \text{ lies in the sextant } i \\ 0 & \text{otherwise.} \end{cases} \quad , \quad i = \{1, 2, 3, 4, 5, 6\}. \tag{3.42}$$

As in steady-state conditions, the term $\mathbf{i}_{ph}$ in (3.41) will be time-dependent; thus, a rotating coordinate transformation can be included to handle the constant values for those variables, as follows:

$$\bar{i}_1 = \mathbf{D}\, \mathbf{S}_T\, \mathbf{i}_{dq}, \tag{3.43}$$

where $\mathbf{S}_T = \mathbf{S}\, \mathbf{T}_{dq}^{-1} = \mathbf{S}\, \mathbf{T}_{dq}^{\mathsf{T}} = \mathbf{T}_{dq}\mathbf{S}^{\mathsf{T}}$, and $\mathbf{i}_{dq} = \mathbf{T}_{dq}\, \mathbf{i}_{ph}$.

Equation (3.43) is general for the three-level diode-clamped converter, since it allows the local averaged NP current to be analyzed for any SVM technique.

The model can be extended to converters with higher numbers of levels. For the general case of an n-level diode-clamped converter with multiple mid points (MPs):

$$\bar{\mathbf{i}}_{MP} = \mathbf{D}\,\mathbf{S}_T\,\mathbf{i}_{dq}\,, \tag{3.44}$$

where $\bar{\mathbf{i}}_{MP} = \begin{bmatrix} \bar{i}_{n-2} & ... & \bar{i}_2 & \bar{i}_1 \end{bmatrix}^{\mathsf{T}}$, and

$$\mathbf{D} = \begin{bmatrix} \displaystyle\sum_{\substack{i,j,k \neq n-2 \\ i \geq j \geq k}} \left[d_{(n-2)jk} - d_{i(n-2)(n-2)} \right] & \displaystyle\sum_{\substack{i,j,k \neq n-2 \\ i \geq j \geq k}} \left[d_{i(n-2)k} - d_{(n-2)j(n-2)} \right] & \displaystyle\sum_{\substack{i,j,k \neq n-2 \\ i \geq j \geq k}} \left[d_{ij(n-2)} - d_{(n-2)(n-2)k} \right] \\ \vdots & \vdots & \vdots \\ \displaystyle\sum_{\substack{i,j,k \neq 2 \\ i \geq j \geq k}} \left[d_{2jk} - d_{i22} \right] & \displaystyle\sum_{\substack{i,j,k \neq 2 \\ i \geq j \geq k}} \left[d_{i2k} - d_{2j2} \right] & \displaystyle\sum_{\substack{i,j,k \neq 2 \\ i \geq j \geq k}} \left[d_{ij2} - d_{22k} \right] \\ \displaystyle\sum_{\substack{i,j,k \neq 1 \\ i \geq j \geq k}} \left[d_{1jk} - d_{i11} \right] & \displaystyle\sum_{\substack{i,j,k \neq 1 \\ i \geq j \geq k}} \left[d_{i1k} - d_{1j1} \right] & \displaystyle\sum_{\substack{i,j,k \neq 1 \\ i \geq j \geq k}} \left[d_{ij1} - d_{11k} \right] \end{bmatrix}$$

$$\forall i,\, j,\, k \in \{0,\, 1,\, 2,\, ...,\, n-1\}.$$

3.2.6.1. Limits of NTV Modulation

In this section, the limits of the ability to control the NP balance in the NTV modulation technique are analyzed. Such limits will be determined by selecting the dual vectors such that they reach either maximum or minimum NP current. For instance, for the maximum case, vector 100 will be selected if i_a is positive, and vector 211 if i_a is negative. The situation is similar for vectors 110 and 221, taking into account the direction of i_c. The minimum NP current is found by the opposite reasoning.

In Fig. 3.22, the waveforms that limit the maximum and minimum local averaged NP current are shown for some examples. These waveforms are normalized by the amplitude of the AC phase currents ($\hat{I}$), which are in steady-state conditions. Different lengths of the reference vector have been considered for a zero-degree current phase angle ($\varphi = 0^{\circ}$).
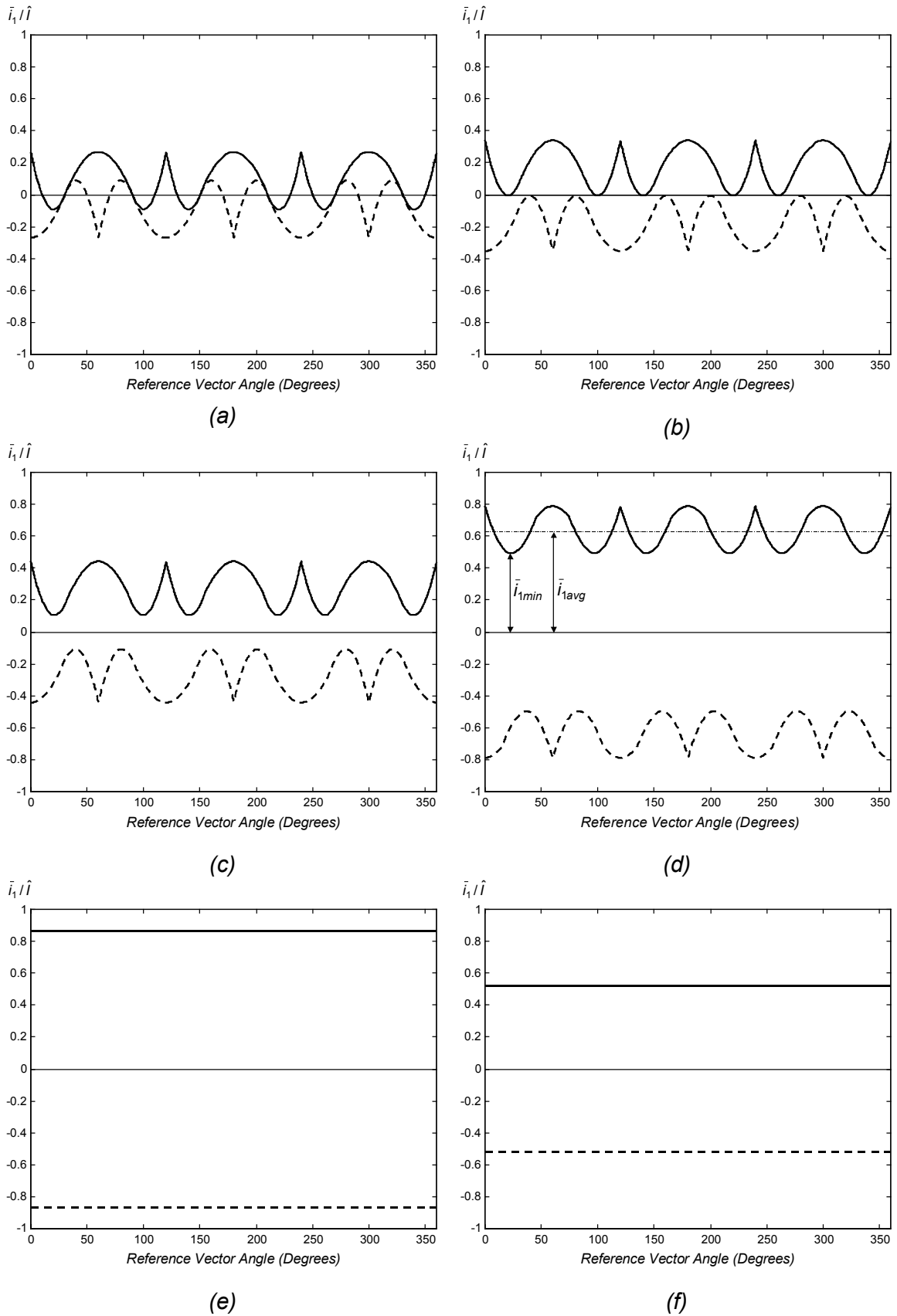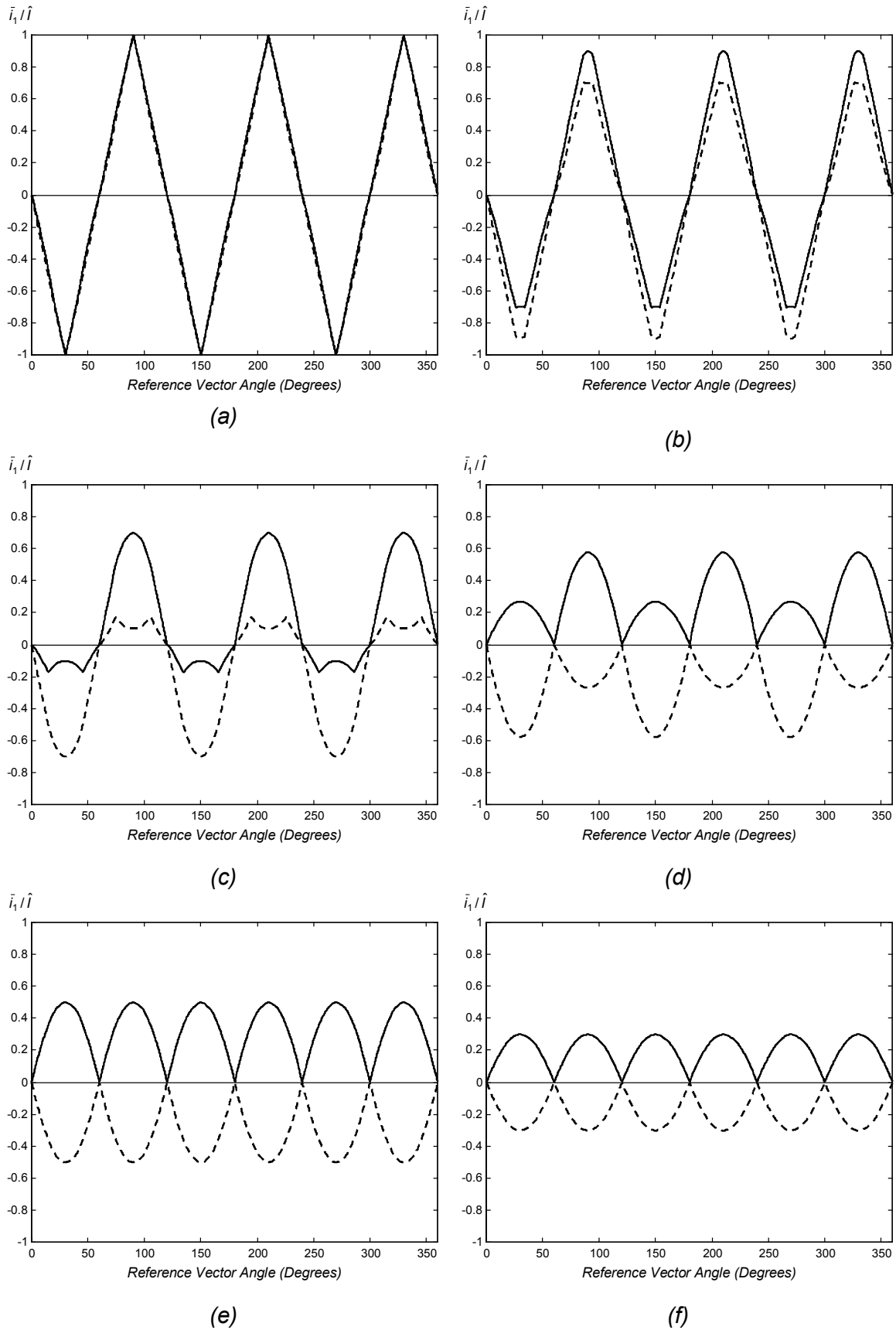
Fig. 3.22. *Normalized maximum (solid line) and minimum (dashed line) local averaged NP current. Examples given for purely resistive load ($\varphi=0^o$):*
(a) m=1; (b) m=0.9541; (c) m=0.9; (d) m=0.7; (e) m=0.5; and (f) m=0.3.

For the case in which *m*=1 in Fig. 3.22, the upper waveform that limits the maximum NP current dips into negative values. Therefore, it is not possible to achieve positive NP current values for some positions of the reference vector when this is required for voltage-balance control. Similarly, this stipulation also exists for the lower waveform that limits the minimum NP current, since both waves are symmetric. Under those conditions, the local averaged value of this current over a modulation period cannot be confined to zero. As a result, a low-frequency harmonic appears in the NP current, and this eventually becomes NP voltage oscillations.

In contrast, for the case in which *m*=0.9541, the upper local averaged NP current waveform always consists of positive values (the lowest NP current waveforms will not be considered henceforth, since they are symmetric). Therefore, the current is always controlled and balance is achieved. In fact, this length of the reference vector is the limiting case for the unity PF, because the minimum value of the upper NP current waveform is zero. For smaller amplitudes of the reference vector, the NP current is always controlled. Those waveforms also provide information as to the spare NP current available for achieving balance.

In Fig. 3.23, the load is considered to be purely inductive. For this case, full NP current control is not achieved for reference vector lengths greater than *m*=0.5774.

Fig. 3.23. *Normalized maximum (solid line) and minimum (dashed line) local averaged NP current. Examples given for purely inductive load (φ=-90º):*
(a) m=1; (b) m=0.9; (c) m=0.7; (d) m=0.5774; (e) m=0.5; and (f) m=0.3.

The three-dimensional diagram in Fig. 3.24(a) shows the minimum values from the highest NP currents' waveforms ($\bar{i}_{1min}$). The area above the black (zero) plane is where the minimum value is positive; therefore, full control for the NP current can always be achieved. The area below this plane shows negative values for the NP current waveforms, which means that a third-order harmonic will appear in the NP current.

On the other hand, Fig. 3.24(b) shows the averaged value from those waveforms, worked out over a whole line period ($\bar{i}_{1avg}$). Since these values are always positive, the entire surface is above the zero plane. Hence, despite the low-frequency ripple, the control always retains the ability to keep those oscillations at one half the level of the DC-link voltage. This figure also provides information about how quickly the NP can be re-balanced after an unbalanced transition.
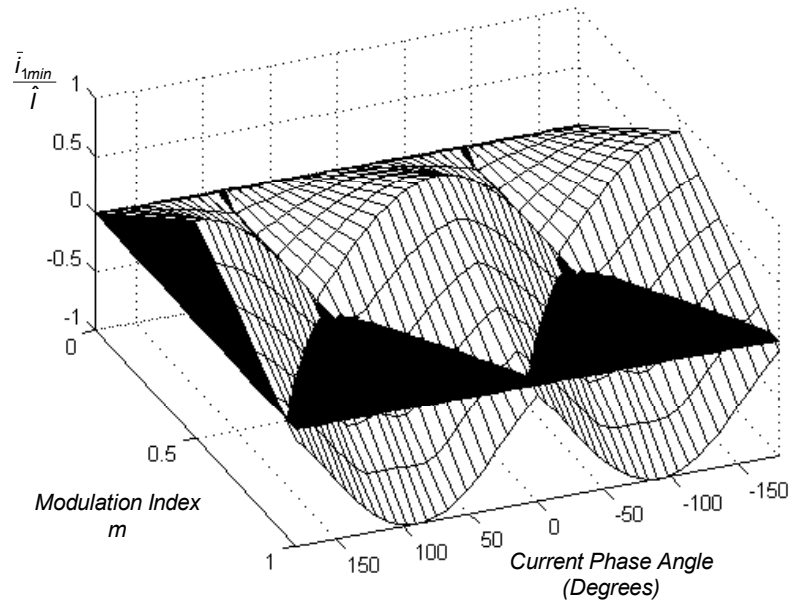
(a)
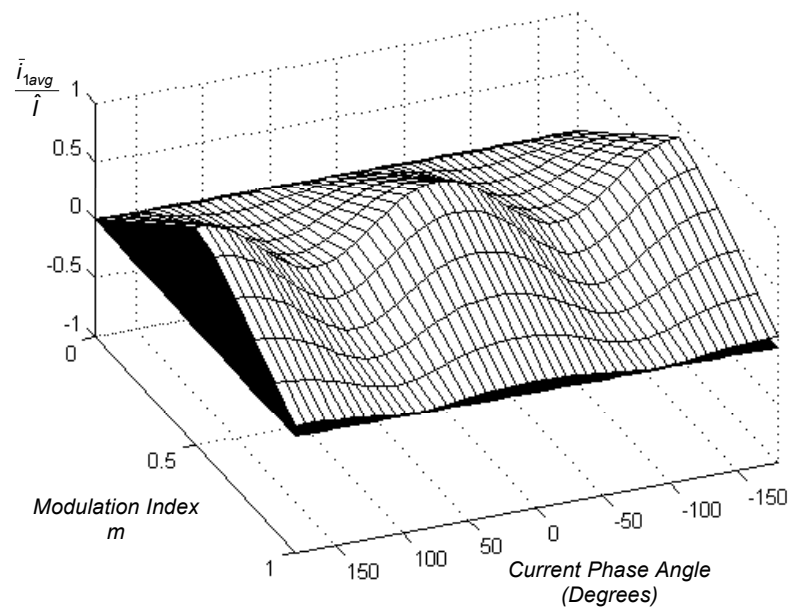
(b)

Fig. 3.24. *(a) Minimum local averaged values and (b) whole-line-period averaged values of the upper NP current waveforms.*

The surfaces in Fig. 3.24 contain symmetries with respect to the current phase angles 0° and 180°. For any modulation index,

$$\bar{\bar{i}}_{1min}, \ \bar{\bar{i}}_{1avg} = f(\pm\varphi) = f(180^o \pm \varphi), \tag{3.46}$$

or

$$\bar{\bar{i}}_{1min}, \ \bar{\bar{i}}_{1avg} = f(\pm PF), \quad \text{where } PF = \cos\varphi. \tag{3.47}$$

Fig. 3.25 shows some sections from Fig. 3.24(a) where the curves are given for different PFs. One conclusion is that the unity PF is the most favorable case, because it can contribute more current to the NP balance. On the other hand, the closer the modulation index is to 0.5, the better the NP current control. This is logical since the duty cycles of the short vector are higher in those conditions, and, as a consequence, they have more NP current control.
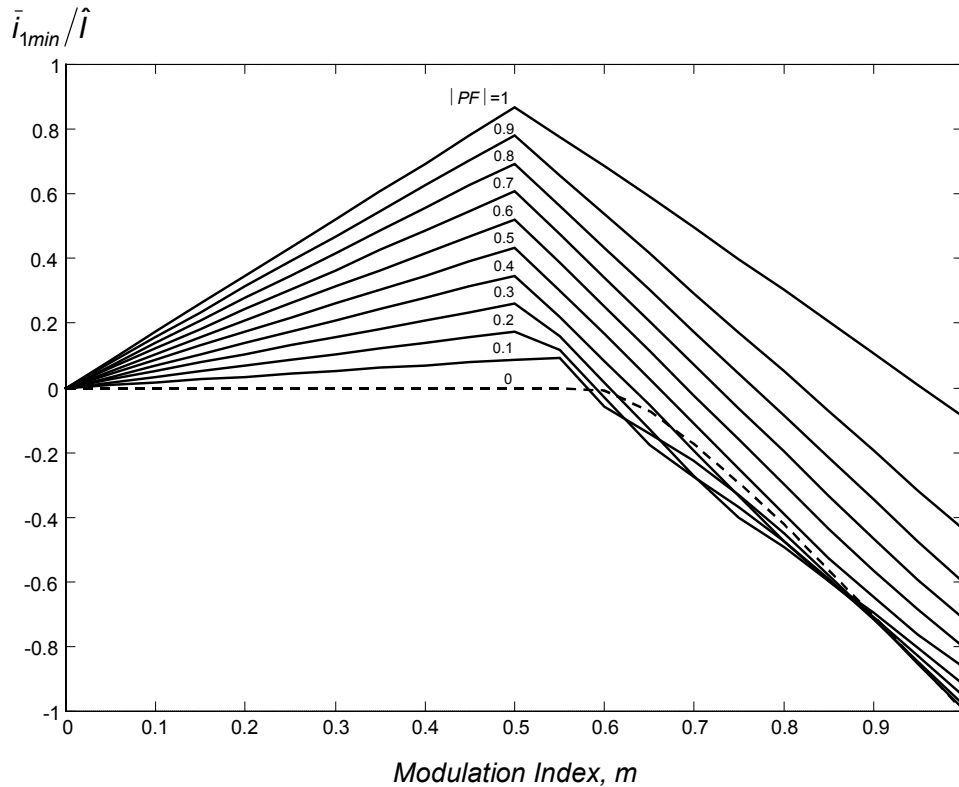
Fig. 3.25. *NP current availability for different PF values.*

The knowledge of the NP current availability will be useful for analyzing the case in which two three-level converters are connected back-to-back, so that they can share the NP-balancing task. This analysis is performed in Chapter 6.

Fig. 3.26 shows the maximum NP voltage ripple that could occur as a result of the NP current. The normalized amplitude of the ripple ($\Delta V_{NPn}/2$) is defined as follows:

$$\frac{\Delta V_{NPn}}{2} = \frac{\Delta V_{NP}/2}{I_{RMS}/f\,C} \, . \tag{3.48}$$

Figure 3.26(b) provides helpful information for determining the value of the capacitors for a practical application. For example, assuming the worst operating

conditions of unity modulation index (m=1) and current angle φ=-84° or φ=+96°, the maximum normalized ripple is:

$$\frac{\Delta V_{NPn}}{2} = \frac{\Delta V_{NP}/2}{I_{RMS}/f\,C} = 0.02973 . \tag{3.49}$$

If the values were I_{RMS}=220 A, f=50 Hz, and C=550 µF, the amplitude of the NP voltage ripple would be:

$$\frac{\Delta V_{NP}}{2} = \frac{\Delta V_{NPn}}{2}\frac{I_{RMS}}{f\,C} = 0.02973\,\frac{220}{50\cdot 550\cdot 10^{-6}} = 237.8\ V . \tag{3.50}$$

It can be observed that the value of the total DC-link voltage V_{DC} does not affect the NP voltage ripple. This statement is true under the assumption that the AC currents are not affected by the NP oscillation, which can be acceptable in the case of relatively small NP-voltage amplitudes. Significant inductive loads contribute to make output currents less sensitive to NP voltage oscillations.
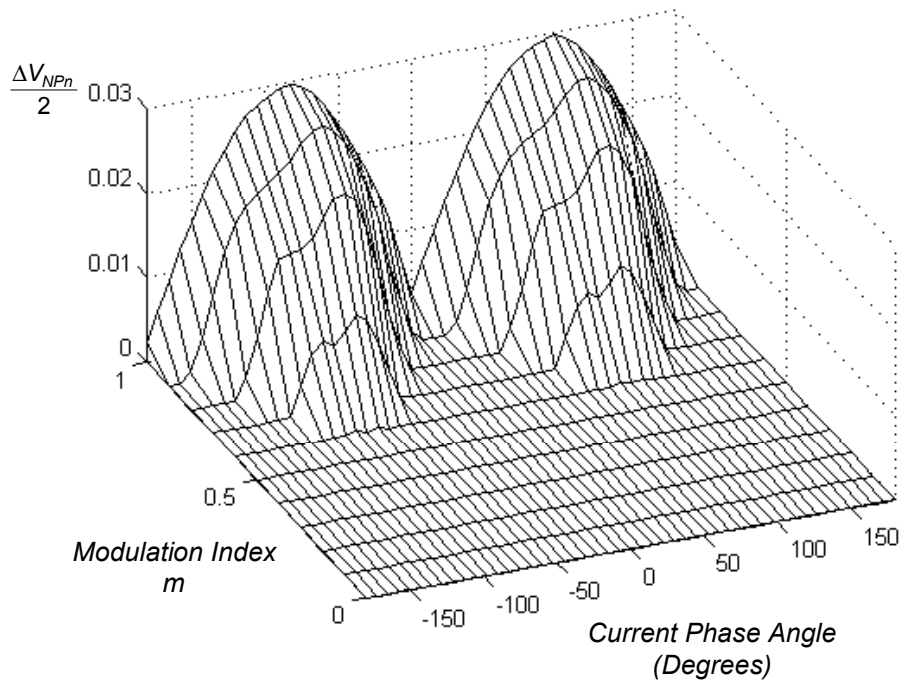
(a)
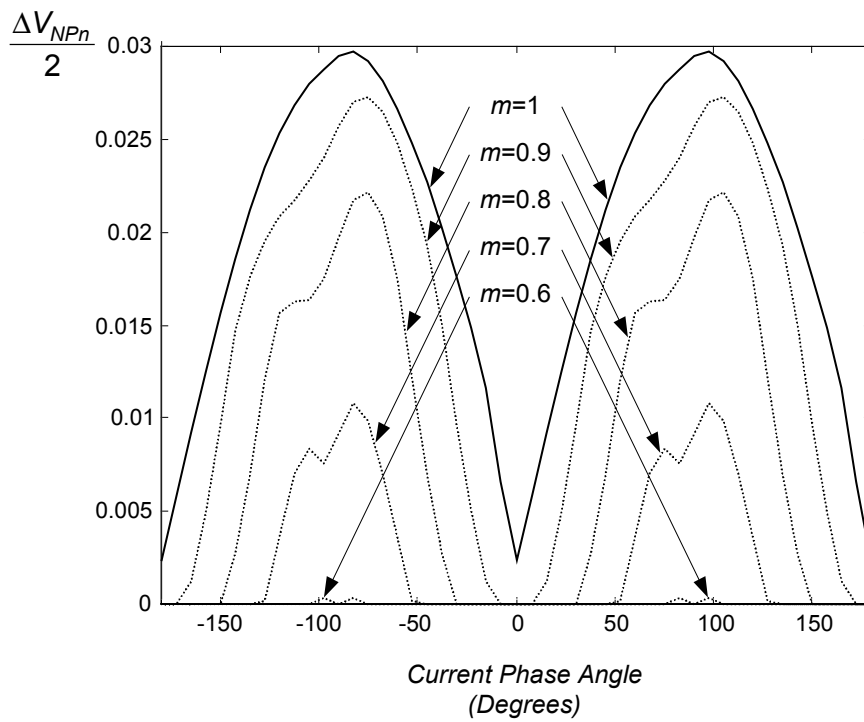
(b)

Fig. 3.26. *Normalized NP voltage ripple for NTV.*

3.2.6.2. Limits of Symmetric Modulation

The NP current limits of the symmetric modulation technique will be determined in a manner similar to the process described for NTV modulation. To achieve maximum and minimum NP averaged current, the control variables x_1 and x_2 will be fixed to extreme values: $x_1, x_2 = \{-1, 1\}$. Thus, only three vectors will be used for the modulation.

Waveforms of the local averaged NP current are given for different lengths of the reference vector. For the examples in Figs. 3.27 and 3.28, the current angles have been considered to be zero and an inductive ninety degrees, respectively.

The maximum length of the reference vector to achieve full control of the NP voltage with a current angle of zero is the same as for the NTV modulation technique (*m*=0.9541). However, for a purely reactive load angle, the maximum value is smaller (*m*= 0.5) than for NTV modulation.

The symmetric modulation technique has less NP current control than NTV modulation. Although symmetric modulation usually uses four vectors per modulation cycle, only three vectors are used when the NP voltage imbalance is at the edge of or beyond the control limits. Furthermore, in contrast with NTV modulation, only one short vector per modulation cycle is selected according to NP voltage-balancing requirements. The other short vector is assigned, depending on whether the normalized reference vector is above or below thirty degrees. Thus, as compared with NTV modulation, there is one fewer variable for the NP current control when the reference vector lies in the inner regions.

The normalized amplitude of the low-frequency NP ripple is presented in Fig. 3.30. This figure shows the existence of this ripple for an extensive operating area. Nevertheless, the maximum value of the ripple is the same than with NTV ($\Delta V_{NPn}/2 = 0.02973$) and it is produced under the same operating conditions (*m*=1 and current angle φ=-84° or φ=+96°).
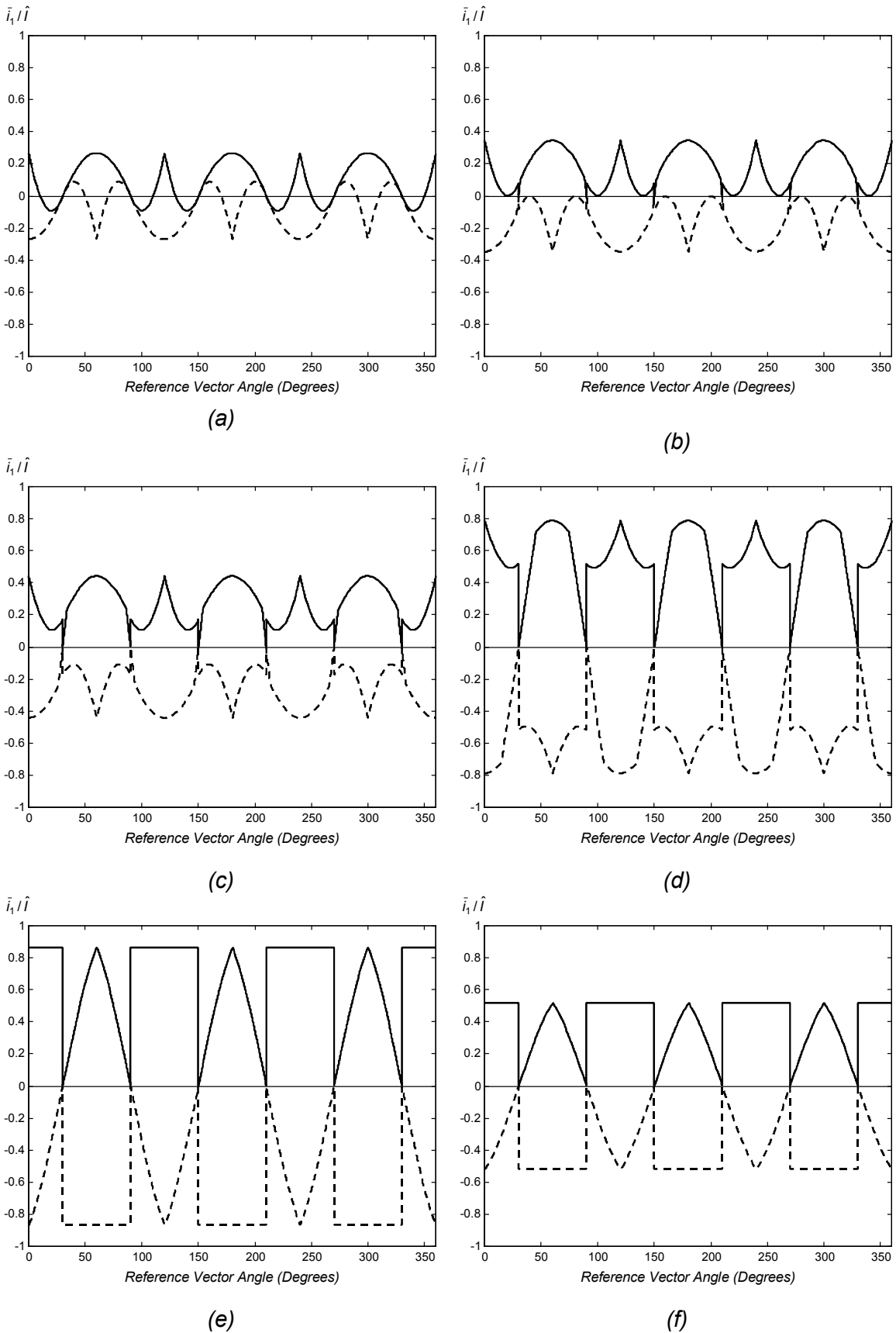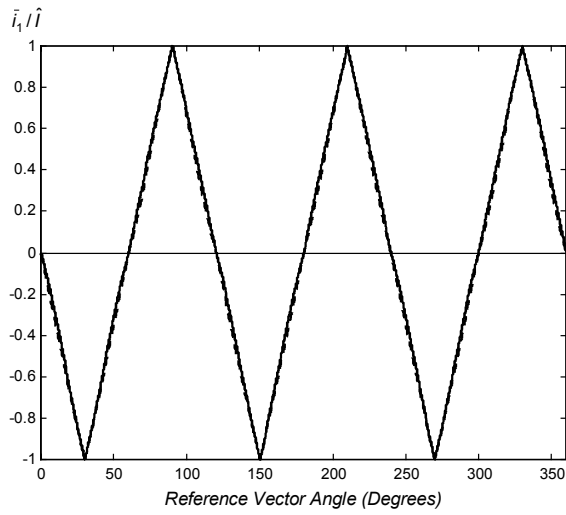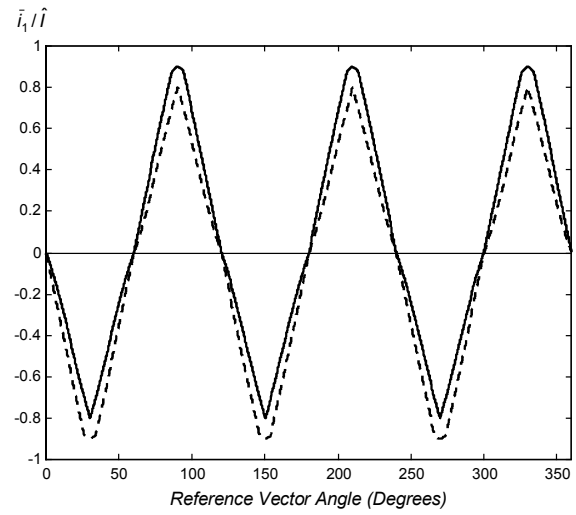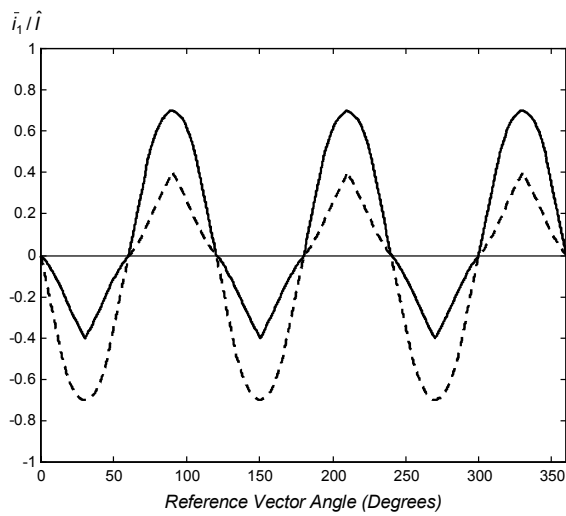
Fig. 3.27. Normalized maximum (solid line) and minimum (dashed line) local averaged NP current for symmetric modulation. Examples given for a purely resistive load ($\varphi=0^o$): (a) m=1; (b) m=0.9541; (c) m=0.9; (d) m=0.7; (e) m=0.5; and (f) m=0.3.

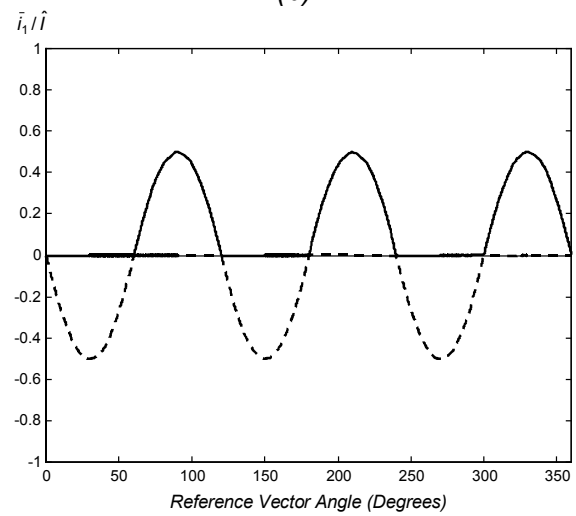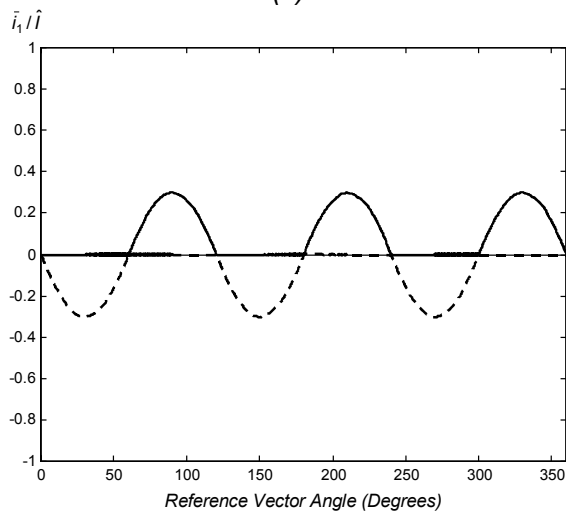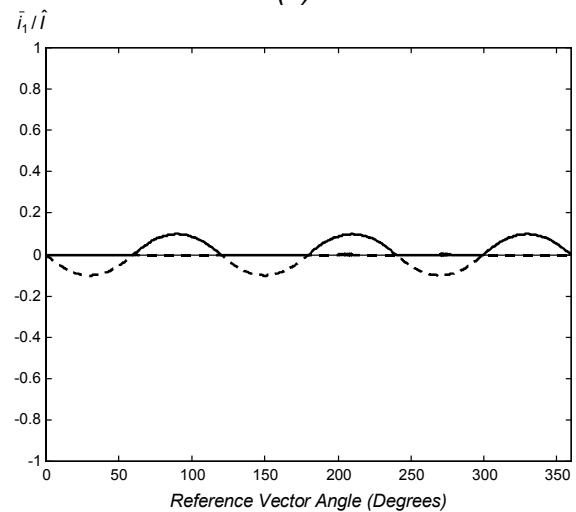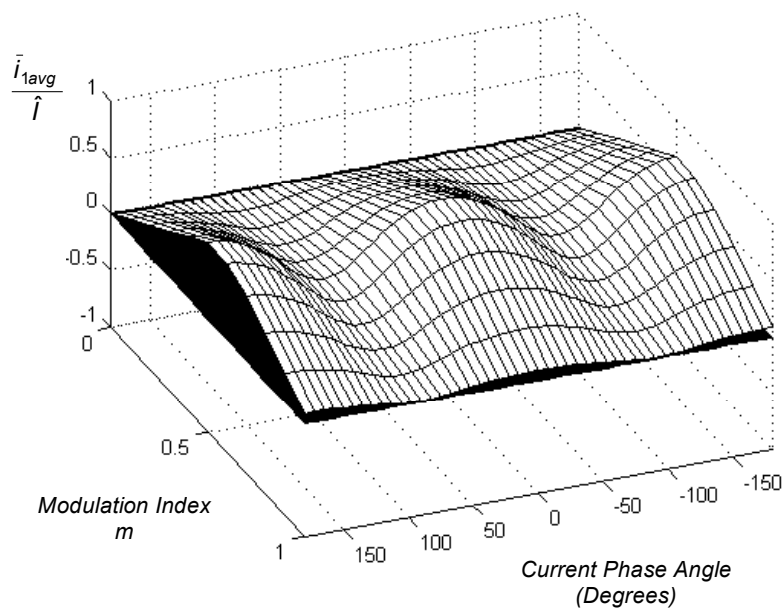**Fig. 3.28.** *Normalized maximum (solid line) and minimum (dashed line) local averaged NP current for symmetric modulation. Examples given for a purely inductive load (φ=-90º): (a) m=1; (b) m=0.9; (c) m=0.7; (d) m=0.5; (e) m=0.3; and (f) m=0.1.*

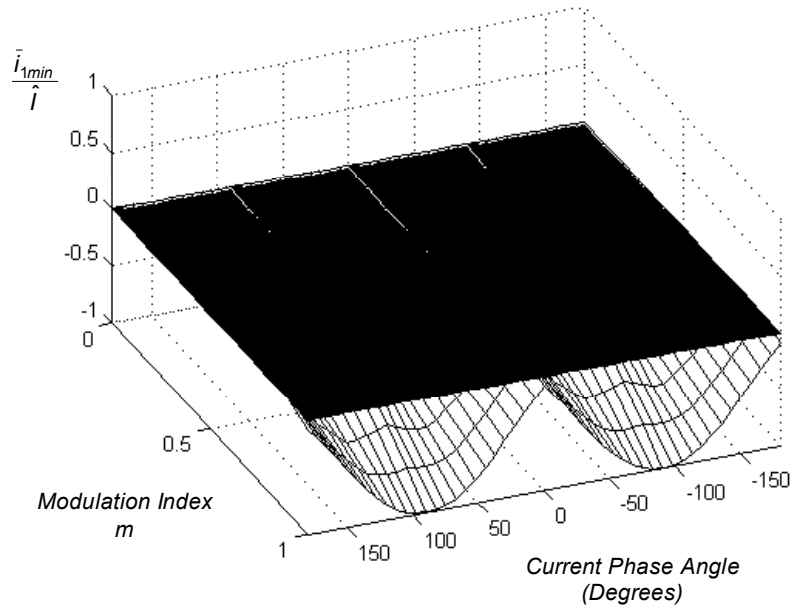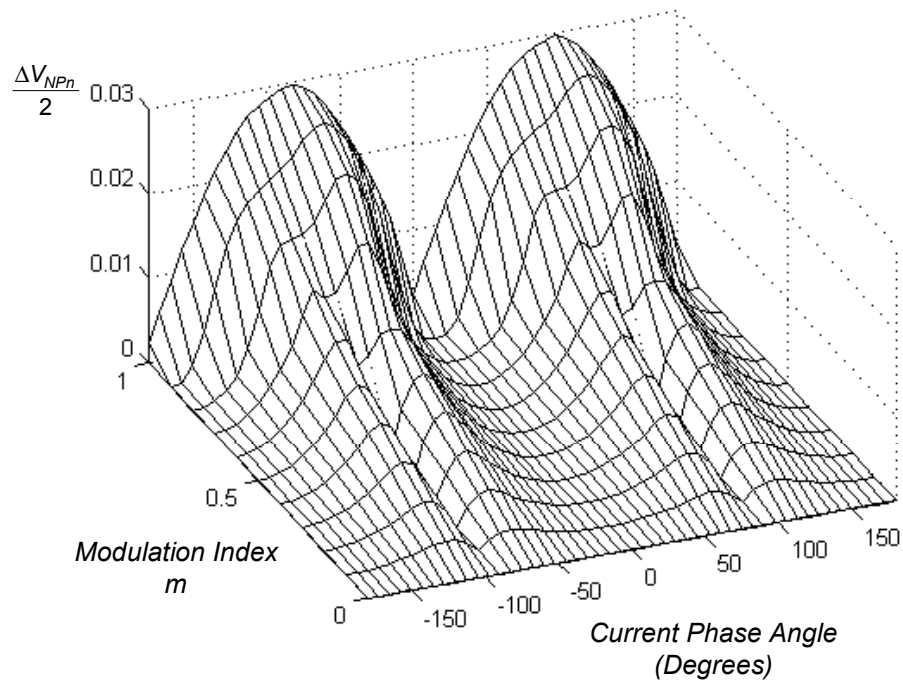$$\frac{\bar{i}_{1min}}{\hat{I}}$$
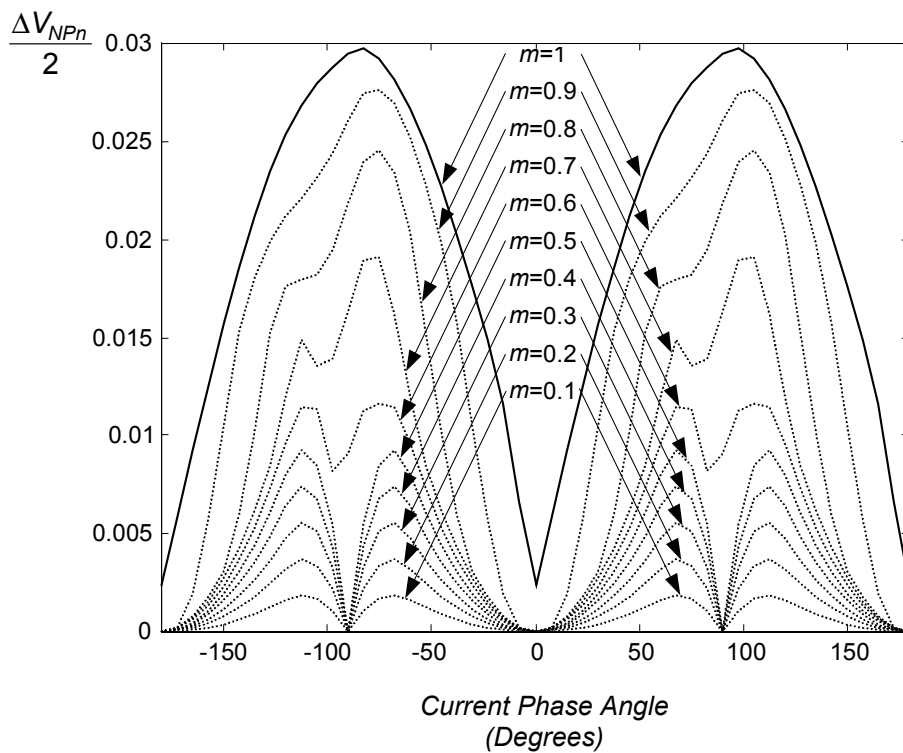
(a)

$$\frac{\bar{i}_{1avg}}{\hat{I}}$$

(b)

Fig. 3.29. *(a) Minimum local averaged values and (b) whole-line-period averaged values of the upper NP current waveforms.*

(a)

(b)

Fig. 3.30. *Normalized NP voltage ripple for symmetric modulation.*

3.2.7. Modulation Algorithm

Fig. 3.31 summarizes the steps required for the application of the proposed fast SVM algorithm in a DSP. This diagram considers the NTV modulation technique, however it can be easily adapted to symmetric modulation with slight changes.
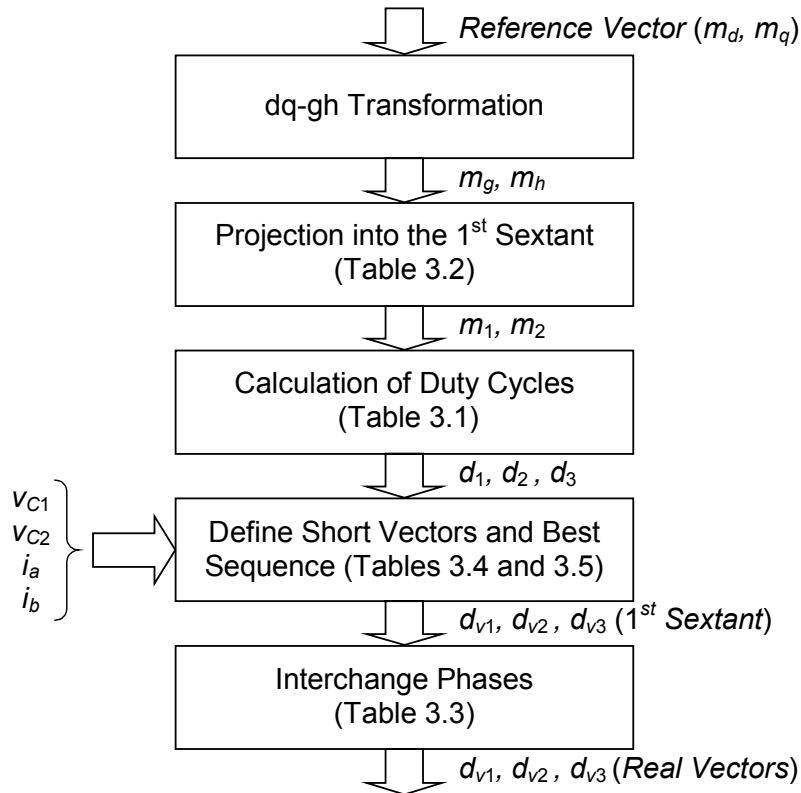
Reference Vector (m_d, m_q)

| dq-gh Transformation |

m_g, m_h

| Projection into the 1st Sextant (Table 3.2) |

m_1, m_2

| Calculation of Duty Cycles (Table 3.1) |

d_1, d_2, d_3

v_{C1}
v_{C2}
i_a
i_b

| Define Short Vectors and Best Sequence (Tables 3.4 and 3.5) |

d_{v1}, d_{v2}, d_{v3} (1st *Sextant*)

| Interchange Phases (Table 3.3) |

d_{v1}, d_{v2}, d_{v3} (*Real Vectors*)

Fig. 3.31. *General diagram of the SVM algorithm.*

The short time required for processing this modulation algorithm hinges on these following points.

- The dq-gh transformation directly translates the control variables given in dq coordinates into a non-stationary coordinate system, providing useful variables for the modulation.

- All of the calculations are made in the first sextant; therefore the total number of regions involved is divided by six.

- Most of the operations required are based on products and comparison operations, which are quickly processed by a DSP.

3.2.8. Experimental Results

The proposed SV-PWM algorithm has been programmed into the 32-bit floating-point digital processor (Sharc ADSP 21062) of the SMES system. Its instruction processing time of 25 ns allows the algorithm to be processed in less than 4 μs. The modulation period of the three-level converter is T_m=50 μs (f_m=20 kHz). An asynchronous motor is connected as a load.

In Fig. 3.32, the DC-link voltage is provided by a DC power supply adjusted to 60 V. This figure shows a line-to-line output voltage and two output currents for the modulation index m=0.9. Fig. 3.33 shows the same variables for the case when m=0.4. These experimental results have been also verified by simulation. An R-L load is used for the simulation results, so the values have been adjusted to achieve the same amplitude and phase angle for the output currents.

Fig. 3.34 shows the voltages of the two DC-link capacitors, a low-pass-filtered line-to-line output voltage and an output phase current. The capacitors are forced to have a permanent voltage imbalance by means of two DC power supplies. The upper one is adjusted to 60 V and the lower one to 10 V. When the NP connection is released, the modulation process itself controls the voltage balance. As the selection of dual vectors is properly made, balance is achieved.
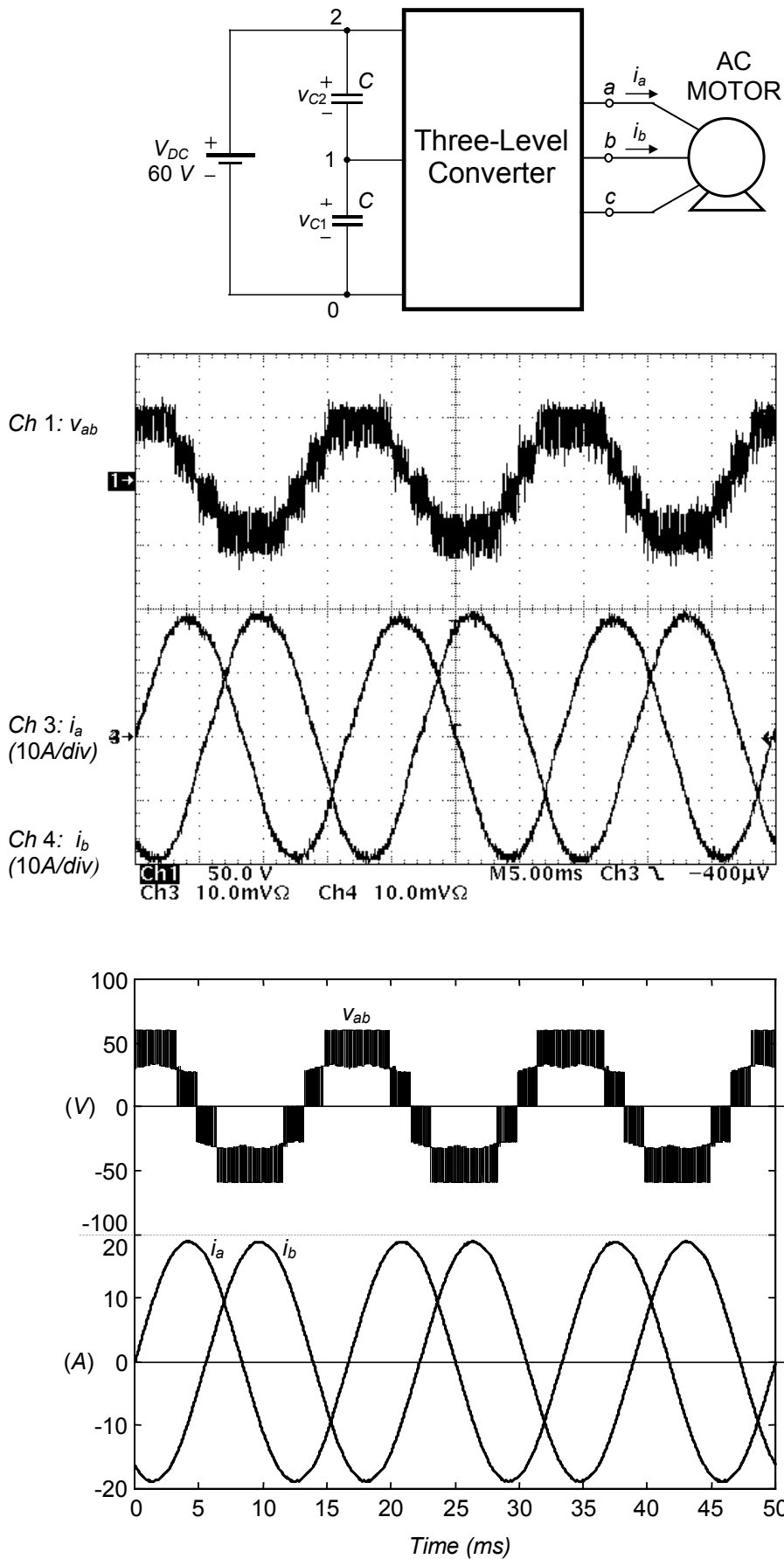
Fig. 3.32. *Line-to-line voltage (v_{ab}) and output currents (i_a and i_b), for modulation index m=0.9.*
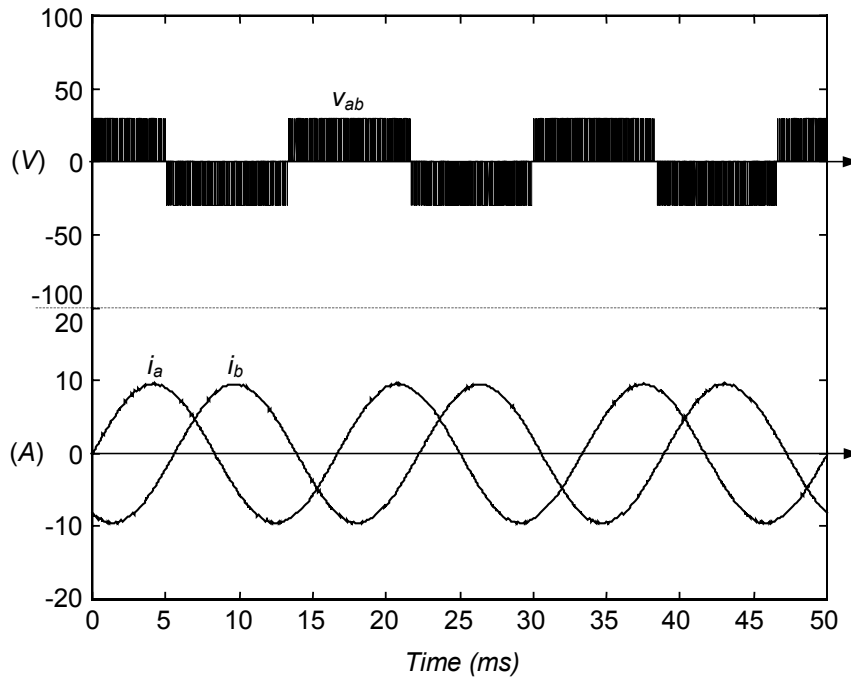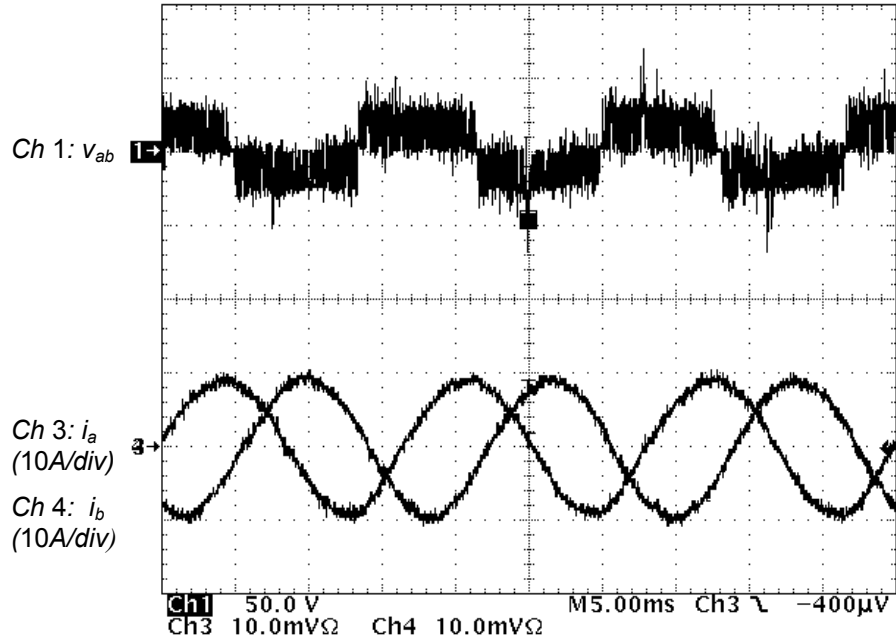
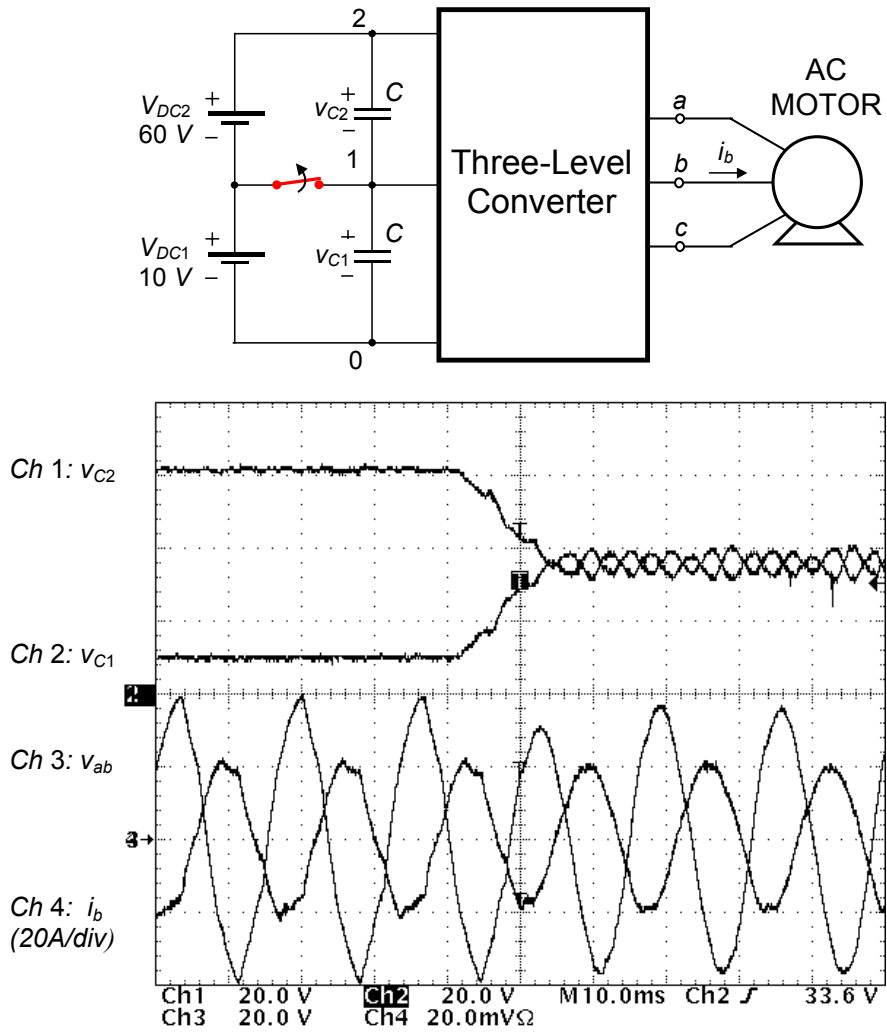**Fig. 3.33.** *Line-to-line voltage (v_{ab}) and output currents (i_a and i_b), for modulation index m=0.4.*

Fig. 3.34. *DC-link voltages (v_C1 and v_C2), filtered line-to-line voltage (v_ab) and output phase current (i_b). The NP voltage is released to be controlled by the modulation itself.*

3.3. Conclusions of the Chapter

Some general modulation issues are presented in this chapter. The duty cycles are calculated by projections of the reference vector, and by the dq-gh transformation, which translates the control variables into a pair of components very useful for the modulation. An equivalent reference vector is used for processing calculation in the first sextant. This equivalent vector has the propriety that interchanging the final states of the phase legs automatically generates the original reference vector.

For the case of the three-level converter, two modulation techniques are analyzed: NTV and symmetric modulation. Assuming a modulation period much smaller than the line period (T_m<<T), the first method presents certain advantages, such as a lower switching frequency and an extended operation area without low-frequency NP voltage oscillations. Better performance than NTV is obtained with symmetric modulation when dealing with large modulation periods, from the standpoint of output voltage spectra and NP voltage ripple. Some practical graphics are presented to obtain the amplitude of the low-frequency NP voltage ripple for both modulation strategies. This information is very useful for the calculation of the values of the DC-link capacitors.

NTV modulation has been implemented in the DSP of the SMES system. This processor has an instruction time of 25 ns, and the algorithm requires less than 4 µs to be processed. As all of the calculations are made in the first sextant, only four regions must be considered for the modulation, instead of the twenty-four that comprise the whole diagram. Therefore, most of the operations can be realized by just checking some conditions of small tables. Optimal sequences of vectors are applied in order to achieve minimal switching frequencies for the devices of the bridge. The criterion used for the selection of the short vectors helps the NP voltage to achieve balance. As the modulation process itself performs the voltage-balancing task, the control stage is relieved of this duty.